EFFECT OF YTTRIA CONTENTS AND GRAIN SIZES ON FATIGUE BEHAVIOR OF YTTRIA-CONTAINING TETRAGONAL ZIRCONIA POLYCRYSTALS(Y-TZP)

Masahiro ASHIZUKA
Kyushu Institute of Technology, Department of Materials Science and Engineering, 1-1, Sensui-cho, Tobata-ku, Kitakyushu, 804 JAPAN.
Yoshitaka KUBOTA
Tosoh Corporation, Advanced Materials Research Laboratory, 2743-1, Hayakawa, Ayase 252 JAPAN.

ABSTRACT

Fatigue behavior of tetragonal zirconia polycrystals containing yttria (Y-TZP) was measured by static and dynamic fatigue technique. The crack growth parameters N at room temperature were 67.3 to 104 for 2mol%Y_2O_3-TZP, 41.0 to 53.6 for 3mol%Y_2O_3-TZP and 31.7 to 46.1 for 4mol%Y_2O_3-TZP. The N values of TZP containing 2 ,3 and 4mol%Y_2O_3 in the grain size groups of more than 1μm at 250℃ became less than 10 indicating remarkable fatigue. While, in the case of the grain size group of 0.5μm at 250℃, the N value for 3mol%Y_2O_3-TZP was 50.5 indicating little fatigue, but the N values for 2 and 4mol%Y_2O_3-TZP decreased until 21.9 and 32.3 to 40.9, respectively. The monoclinic zirconia on fracture surface increased with increasing grain size at a constant Y_2O_3 and decreased with increasing Y_2O_3 contents at a constant grain size. The fatigue fracture surfaces were observed on the fracture surface of 3mol%Y_2O_3-TZP with the grain size of about 1μm or above, and 2mol%Y_2O_3-TZP with the grain size of 0.5μm or above at 250℃.

1. INTRODUCTION

Tetragonal zirconia polycrystals containing yttria (Y-TZP) in which the tetragonal zirconia is metastable at ambient temperature have been of considerable interest, because they have high strength and fracture toughness.[1)-3)] However, the reported strength values are generally measured at a crosshead speed of 0.5mm/min and it is not evident that such strength values can be maintained in the case of prolonged stress load. Actually many ceramics are known to undergo delayed failure (slow crack growth) at the stress below the reported fracture strength.[4)-8)] While, it is known that the Y-TZP exhibits the degradation of strength by long period of thermal aging at 200℃ to 300℃,[9)] too. That is, it is considered that the degradation of strength of Y-TZP should be classified into that by prolonged stress load (fatigue) and that by tetragonal to monoclinic transformation induced by the reaction with moisture in atmosphere. It is estimated that two mechanism of them is superposed for the degradation of strength when Y-TZP is used at 200° to 300℃. In this study, fatigue behavior of Y-TZP at room temperature and 250℃ was studied by measuring their fracture stress as a function of stressing rate (dynamic fatigue) and the effects of Y_2O_3 content, grain size and temperature to the fatigue

behavior were considered. Furthermore, time-to-failure under a constant stress (static fatigue) was measured for a few specimens and was compared with life time predicted from dynamic fatigue data. In addition, dynamic fatigue behavior was measured in water at room temperature and 95℃, and the effect of water to fatigue behavior was considered.

Our studies about fatigue behavior of yttria-containing tetragonal zirconia polycrystais are reviewed in this paper.[10)-15)]

2. EXPERIMENTAL PROCEDURE

The pressureless sintering TZP (supplied by Tosoh Corporation) were used for this study. Zirconia powder containing 2, 3 and 4 mol%Y_2O_3 prepared by a coprecipitation method was pressed uniaxially at 20MPa and then was compacted isostatically at 300MPa. Their compacted specimens were sintered at 1400° to 1600℃ in air. Their symbols, average grain size and density were listed in Table 1. Specimens were ground with a diamond wheel(#200) to the rectangular bars of 3mm by 4mm by 40mm. Three point bending fixture with a span of 30 mm were used in the dynamic and static fatigue tests. In the dynamic fatigue test, the fracture stress was measured as a function of stressing rates by using a universal testing machine. While, in the static fatigue test, the equipment with lever arm was used. A given load was applied with the lever and the time-to-failure was measured under several applied stresses.

For many glasses and ceramics, it is known that there is a following relationship between crack growth velocity V and stress intensity factor K_I [8) 16)-19)]

$$V = AK_I^N \tag{1}$$

The relationship for zirconia ceramics was reported by L.Li and R.F.Pabst, [20)] P.F.Becker[21) 22)] and R.F.Dauskard et.al.[23) 24)] By assuming Eq.(1), the time-to-failure t_f under a constant applied stress σ (static fatigue technique) was derived[25)-29)]

$$t_f = B_1 \sigma^{-N} \tag{2}$$

Similarly, the fracture stress σ_f at a constant stressing rate $\dot{\sigma}$ (dynamic fatigue technique) was derived[29)-31)]

$$\sigma_f = B_2 \dot{\sigma}^{1/(N+1)} \tag{3}$$

B_2 is related with B_1 by the following equation[25)-29)]

$$B_2^{N+1} = B_1(N+1) \tag{4}$$

That is, time-to-failure t_f can be estimated from dynamic fatigue data by using Eqs.(2), (3) and (4). Where, N is the crack growth parameter for a given materials and environment, and the larger N value is, the larger resistance for fatigue is.

In this study, the dynamic fatigue technique was employed for all specimens, and fatigue behavior was evaluated by the N value. The static fatigue technique was adopted for three specimens(Z2Y-Ⅰ, Z3Y-Ⅱ and Z4Y-Ⅱ) at 250℃. N values and life time predicted from dynamic fatigue data were

compared with these measured by static fatigue technique.

The humidity during their measurements was 50～70%RH. Monoclinic and tetragonal zirconia contents were measured by X-ray methods.[32)-35)]

3. Results and discussion

3.1 Stress-displacement curve[11)]

At room temperature, Stress-displacement curves showed a linear relationship indicating elastic behavior for all specimens. At 250℃, stress-displacement curve showed the elastic behavior at whole stressing rate for 3mol%Y_2O_3-TZP(Z3Y) and 4mol%Y_2O_3-TZP(Z4Y), and at a stressing rate above 3.02 MPa/s (crosshead speed : 0.05 mm/min) for 2mol%Y_2O_3-TZP(Z2Y), too. On the other hand, the stress-displacement relationship of Z2Y deviated from a linear relationship at a stressing rate of 0.301 MPa/s (crosshead speed : 0.005 mm/min) at 250℃. That is, the stress-displacement relationships of 2mol%Y_2O_3-TZP (Z2Y-Ⅰand Z2Y-Ⅱ) at 250℃ showed inelastic bahavior at a slow stressing rate such as 0.301MPa/s. Figs.1 and 2 show the relationship between stress and displacement at a stressing rate of 0.301MPa/s at 250℃ for 2 mol%Y_2O_3-TZP. Figs.1 and 2 showed the relationships for Z2Y-Ⅰ with the grain size of 0.46μm and Z2Y-Ⅱ with grain size of 1.33 μm, respectively. Their relationships deviated from linear one at the higher applied stress. The degree of deviation in Z2Y-Ⅱ with large grain size is larger than that in Z2Y-Ⅰ with small grain size. That is, Z2Y-Ⅱ with the larger grain size(Fig.2) exhibited more remarkable inelastic behaviour than Z2Y-Ⅰ with the smaller grain size(Fig.1).

Fig.3 shows the specimen configulation after measuring stress-displacement relationship. The specimen in Fig.3 corresponds to the curve A in Fig.2. Z2Y-Ⅱ showed the permanent deformation even after unloading. That is, there were specimens not broken even if the displacement at the center support of three point bending equipment reached about 1 mm. Fig.4 shows the lateral surface (photo. a) and tension surface (photo. b) of the specimen in Fig.3 observed by the optical microscope. There were many cracks on the surface of tension side. Their cracks develop perpendicular to the surface. A crack around the center on the surface of tension side is greatly opened and that crack on the lateral side develop to the two-third depth.

The inelastic behavior of partially stabilized zirconia(PSZ) or tetragonal zirconia polycrystals(TZP) has been reported by J.Lankford,[36)-37)] M.V.Swain,[38)-39)] T.B.Troczynski et.al.[40)] and Tsukuma et.al..[41)] Lankford showed that the relationship between stress and strain for MgO-PSZ with grain size of 60μm at room temperature deviated from the linearity at high stress region and exhibited inelastic behavior. He reported that the deformation band was observed on the surface of specimens having been subjected the high stress in the region exhibiting inelastic behavior. Moreover, Swain measured the strength of 9.4mol%MgO-PSZ by four-point-bending test, and reported the elastic behavior for the specimen after

heating treatment for 2 hours at 1100℃ and inelastic behavior for specimen after heating treatment for 40 hours. Furthermore, he observed many microcrack on the tension surface of the specimen after exhibiting inelastic behavior. In addition, R.H.Hannink and M.V.Swain repoted that a deformation band similar to a slip band was formed in vicinity of a Vicker's indent on CaO-partially-stabilized zirconia.[42] The inelastic behavior reported by Swain deviated slightly from linearity in the region of high displacement, while the results obtained in this study showed a stress-displacement curve reaching the maximum stress at a certain displacement. Such a difference for these stress-displacement curve is due not also to the different grain sizes but also to the fact that Swain's result was obtained for the crosshead speed of 0.05mm/min at room temperature, while the result in this study was obtained for the crosshead speed of 0.005 mm/min at 250 ℃.

It is estimated that inelastic behavior reported by Swain and the one obtained in this study relate to stress-induded transformation being responsible for high strength and high toughness of partially stabilized zirconia (PSZ) and teragonal zirconia polycrystals (TZP), and the formation of deformation band relates to plastic deformation resulted from stress-induced transformation that tetragonal zirconia transfer to monoclinic zirconia by applying stress.

3.2 Dynamic Fatigue

3.2.1 Dependece of fracture stress to stressing rate[10)-12) 15)]

The results for tetragonal zirconia polycrystals containing 3mol% Y_2O_3 were shown in Figs.5 and 6. In the case of Z3Y-I (grain size : 0.53μm) at both 20° and 250℃, and Z3Y-II (grain size : 1.06μm) at 20℃, there are linear relationships between $\ell og\,\sigma_f$ -$\ell og\,\dot{\sigma}$ over the whole range of stressing rates. The crack growth parameters N obtained from these slopes are 53.6 at 20℃ and 50.5 at 250℃ for Z3Y-I, and 41.0 at 20℃ for Z3Y-II.
On the other hand, in the case of Z3Y-II at 250℃, σ_f at a stressing rate less than 30.2MPa/s greatly decreased with decreasing stressing rate $\dot{\sigma}$. But the fracture stress σ_f at a stressing rate more than 30.2MPa/s showed a constant value even if the stressing rate $\dot{\sigma}$ increased. The strength exhibiting the constant value above a certain stressing rate is similar to inert strength.[43)-45)] However, the strength of Y-TZP is related to the presence of metastable tetragonal zirconia and may be affected by grain size and atmosphere. Therefore, it is referred to as maximum attained strength σ_{max} in this paper. In the case of Z3Y-II at 250℃, the N value was obtained from the slope below 30.2MPa/s and became a low value of 10.2 indicating the remarkable fatigue phenomena.

The relationship between fracture stress σ_f and stressing rate $\dot{\sigma}$ for tetragonal zirconia polycrystals containing 2mol% Y_2O_3 was shown in Figs.7 and 8. As the relationship between stress and displacement at a stressing rate of 0.301MPa/s showed inelastic behavior at 250℃, the data obtained at a stressing rate more than 3.02 MPa/s is plotted in Fig.7 and 8. There were linear relationships between $\ell og\,\sigma_f$ and $\ell og\,\dot{\sigma}$ over the whole range of

stressing rate at 20℃ for Z2Y-I (grain size : 0.46μm) and Z2Y-II (grain size: 1.33μm), too. On the other hand, fracture stress σ_f at 250℃ for Z2Y-I increased with increasing stressing rate $\dot{\sigma}$ in the range from 3.02 MPa/s to 30.2 MPa/s. However, the fracture stress σ_f showed a tendency to become a constant value over 30.2MPa/s. The N values obtained from these slopes were 104 and 67.3 at room temperature, and 21.9 and 8.7 at 250℃ for Z2Y-I and Z2Y-II, respectively.

The relationships between fracture stress σ_f and stressing rate $\dot{\sigma}$ for tetragonal zirconia polycrystals containing 4mol% Y_2O_3 are showed in Figs. 9 to 12. There were linear relationships between $\ell og\,\sigma_f$ and $\ell og\,\dot{\sigma}$ over the whole range of stressing rate at room temperature and 250℃ for Z4Y-I (grain size : 0.46 and 0.62μm), and at room temperature for Z4Y-II (grain size: 1.33μm). On the other hand, fracture stress σ_f for Z4Y-II and Z4Y-III (grain size : 2.08μm) at 250℃ increased with increasing stressing rate $\dot{\sigma}$ below 3.02MPa/s, but the fracture stress σ_f showed a tendency to became a constant value at a stressing rate above 3.02MPa/s. The N values obtained from these slopes are 31.7 for Z4Y-I a(Grain size : 0.47μm), 32.6 for Z4Y-I c(Grain size : 0.62μm), 46.1 for Z4Y-II and 45.3 for Z4Y-III at room temperature, and 32.3 for Z4Y-I b(Grain size : 0.56μm), 40.9 for Z4Y-I c, 8.7 for Z4Y-II and 4.7 for Z4Y-III at 250℃. The N values obtained from their slopes are summarized in Table 1, too.

Their N values were divided into the grain size groups of about 0.5μm, 1μm and 2μm. Where, the grain size groups of 0.5 and 1 are in the range of grain size of 0.46 to 0.62μm and 1.06 to 1.34μm, respectively. The grain size group of 2μm is 2.08μm alone. Their N values were plotted as a function of Y_2O_3 contents in Fig.13. The N values at room temperature were 67.3 to 104 for 2mol%Y_2O_3-TZP, 41.0 to 53.6 for 3mol%Y_2O_3-TZP and 31.7 to 46.1 for 4mol%Y_2O_3-TZP. That is, the N value at room temperature decreased with increasing Y_2O_3 contents. In the case of grain size group of 0.5μm, the N value at 250℃ was 50.5 for 3 mol% Y_2O_3. However, if Y_2O_3 contents decreases to 2 mol% or increases to 4 mol%, the N value decreases untill 21.9 or 32.3 to 40.9, respectively. On the other hand, in the grain size group more than 1μm, the N value became less than 10 regardless of Y_2O_3 contents.

3.2.2 Monoclinic zirconia contents on fracture surface[12) 15)]

Monoclinic and cubic zirconia are stable phase below 565℃ according to phase diagram of ZrO_2-Y_2O_3 system proposed by H.G.Scott.[46)] However, if grain size of densely sintered TZP is small, tetragonal zirconia which is stable above 565℃ exists in metastable even at room temperature. Such metastable tetragonal zirconia transforms into monoclinic zirconia by fracture.

The monoclinic zirconia contents in the fracture surface after dynamic fatigue test were constant regardless of stressing rate. Their monoclinic zirconia ratio were listed in Table 1, too. Fig.14 shows their monoclinic zirconia ratio as a function of Y_2O_3 contents for grain size groups of 0.5, 1 and 2μm. At a constant Y_2O_3 content, monoclinic zirconia ratio increased with increasing grain size. On the other hand, at a constant

grain size, that ratio decreased with increasing Y_2O_3 contents and became zero at about 4mol% Y_2O_3 in the grain size group of 0.5μm.

Heuer et.al. and Ruhle et.al clarified the fact that the term of surface energy little affects the stability of tetragonal zirconia and the nucleation greatly affects the transformation from tetragonal zirconia to monoclinic one on the basis of observation by transmision electron micrograph.[47)-49)] According to this view, it is necessary to jump an energy barrier of ΔG^* for the metastable tetragonal zirconia to transform to the monoclinic one. Taking the free energy change for trasformation of tetragonal zirconia to monoclinic one as ΔG , Eq.(5) is assumed.[49)-51)]

$$\Delta G^* \simeq (\Delta G)^2 \qquad (5)$$

Taking the change in the chemical free energy as ΔG_c, the change in the strain energy as ΔU_{se}, and the change in the surface energy as ΔU_s , ΔG can be expressed as[50) 52)]

$$\Delta G = -|\Delta G_c| + \Delta U_{se} + \Delta U_s \qquad (6)$$

Assuming that the contribution of surface energy in the transformation of tetragonal to monoclinic is small, ΔU_s can be neglected.

As the free energy change of tetragonal to monoclinic zirconia ΔG_c is negative in the low temperature region, this term is expressed by $-|\Delta G_c|$ in Eq.(6).[51)] $|\Delta G_c|$ increases with reducing temperature and with decreasing Y_2O_3 contents. ΔU_{se} is residual stress due to volume expansion accompanied by phase transformation and anisotropy of thermal expanxsion in the direction of the crystallographic axis of tetragonal zirconia. The effect of residual stress is reduced with increasing Y_2O_3 contents because anisotropy of thermal expanxsion decresases with reducing grain sizes.[53) 54)]

In summery, $(\Delta G)^2$ decreases with increasing Y_2O_3 contents and reducing grain sizes. That is, it is estimated that the transformation of tetragonal to monoclinic zirconia is hindered by increasing Y_2O_3 contents and reducing grain sizes because energy barrier for transformation is higher. The tendency of change of monoclinic zirconia ratio on fracture surface shown in Fig.14 agrees well with the above discussion.

3.2.3 The effect of phase transformation to fatigue behavior[12) 15)]

Swain et. al[39) 55) 56)] have clarified that the relationship between fracture toughness K_{IC} and thickness of transformation zone h was given by following equation.

$$K_{IC} = K^0_{IC} + k_1 \sqrt{h} \qquad (7)$$

where K^0_{IC} is fracture toughness of matrix in the case that stress induced phase transformation is not occurred and k_1 is a constant value. The relationship between K_{IC}, fracture stress σ_f and crack length c be expreesed as

$$K_{IC} = Y \sigma_f \sqrt{c} \qquad (8)$$

If it is assumed that crack length c is constant, Eq.(9) is derived from Eqs.(7) and (8).

$$\sigma_f = \sigma_0 + k_2 \sqrt{h} \qquad (9)$$

where, σ_0 is materials strength in the case that stress induced phase

transformation is not occurred, and k_2 is a constant value. On the other hand, the relationship between critical transformation stress σ_c and thickness of transformation zone h is given by following equation.[56]

$$\sigma_c = k_3 / \sqrt{h} \qquad (10)$$

where, k_3 is a constant value.

Fiq.15 shows the schematic relationship between Eqs.(9) and (10). In the range that $\sqrt{h}$ is smaller than the intersect point A_1 of two curves representing Eqs.(9) and (10), Eqs.(7), (8) and (9) is applied (flaw limited strength region). If the relationship between σ_f and $\sqrt{h}$ is in this region, fracture stress σ_f increses with increasing fracture toughness K_{IC}, namely with increasing $\sqrt{h}$, and t→m transformation acts as resistance to fatigue. On the other hand, in the range that $\sqrt{h}$ is larger than the intersect point A_1, fracture stress σ_f decreases along the curve representing Eq.(10) with increasing fracture toughness K_{IC}, namely with increasing $\sqrt{h}$, because critical transformation stress σ_c become lower than fracture stress σ_f estimated from Eq.(9) (transformation limited strength region). That is, t→m transformation is facilitated by increasing $\sqrt{h}$ and fracture stress σ_f reduces with increasing $\sqrt{h}$. By elevating temperature from 20° to 250℃, intersect point A_1 of two curves representing Eqs.(9) and (10) shifts to A_2 indicating a lower value.

It is estimated that fatigue behavior of Y-TZP which stress induced transformation is basic strengthening and toughening mechanism relates to t→m transformation. Fig.16 plots fracrure stress σ_f at a crosshead speed of 0.005mm/min (corresponding to a stressing rate of 0.336MPa/s at room temperature and 0.301MPa/s at 250℃) as a function of $\sqrt{h}$. Fracture toughness σ_f at room temperature gradually increased with increasing $\sqrt{h}$ and a proportion of the increase was larger in TZP with small grain size. Fracture stress σ_f at 250℃ was approximately constant below transformation zone size h of 0.063μm (corresponding to monoclinic zirconia contents of 4%) for grain size group of 0.5μm and gradually increased with increasing h above h of 0.063μm. The σ_f for grain size group of 1μm was almost constant below h of 1μm and remarkably decreased with increasing h above h of 1μm.

Fig.17 shows relationship between crack growth parameter N and $\sqrt{h}$. The N value at the room temperature increased with increasing $\sqrt{h}$ regardless of grain size below transformation zone size h of 0.6μm. However, the tendency of increase of the N value by increasing h above h of 0.6μm was influenced by the grain size of the specimen, and the tendency of increase for grain size group of 0.5μm became more remarkable than that tendency for grain size group of 1μm. The N value at 250℃ for grain size group of 0.5μm was similar to that at room temperature below h of 0.6μm and gradually increased with increasing h . However, the N value remarkably decreased with increasing h above h of 0.6μm. The N value at 250℃ for grain size group of 1μm showed a constant value of average 9.2 regardless of the transformation zone size h.

Fatigue behavior of Y-TZP is considered by comparing Figs.16 and 17 with Fig.15. It is estimated that the results at room temperature in Figs.15 and 16 is in the range of flaw limited strength. Consequently,

the N value is considered to increase with increasing the quantity of phase trsnsformation because phase trasformation of zirconia (t→m transformation) acts as resistance to fatigue.

As already described, the intersect point A_1 of two curves representing Eqs.(9) and (10) reduces to the A_2 point by elevating temperature to 250℃. It has become apparent from Fig.17 that N values at 250℃ for the grain size group of 0.5μm would increase with increasing transformation zone size h below h of 0.6μm and remarkably decrease with increasing h above h of 0.6 μm. It is assumed that abrupt change in the relationship of N and $\sqrt{h}$ at h of 0.6μm in Fig.17 shows that the point of h at 0.6μm corresponds to A_2 point in Fig.15. That is, in the case of small grain size group as 0.5μm, even at 250℃, t→m transformation below h of 0.6μm is considered to act as resistance to fatigue and N value increases with increasing the quantity of t→m transformation because the relationship of N and h is in the region of flaw limited srength. On the other hand, N value at 250℃ above h of 0.6μm remarkably decreased with increasing the quantity of t→m transformation because the relationship between N and $\sqrt{h}$ was in the region of transformation limited strength . If grain size become larger as 1 and 2μm, A_1 point in Fig.15 shifts to less value than A_2 point and so that the relationship between N and $\sqrt{h}$ become in the region of transformation limited strength even at thickness of transformation zone h less than 0.6μm. That is, the N value at 250℃ for grain size group of 1 and 2μm in Fig.17 is cosidered to become much small, because all data for grain size group of 1 and 2μm at 250℃ are in the region of transformation limited strength.

3.3 Static Fatigue[10) 13) 15)]

Fig.18 shows the relationship between applied stress σ and time-to-failure t_f for 3 mol% Y_2O_3-TZP with a grain size of 1.06μm(Z3Y-Ⅱ) at 250℃. There is a linear relationship between $\ell og\sigma$ and $\ell og t_f$ and N values are obtained from the slope, too. The N value measured by static fatigue technique was 10.7 and agred well with that obtained from dynamic fatigue data. However, the average life time measured by the static fatigue technique was 4 to 6 times the life time predicted from dynamic fatigue data.

The relationship between $\ell og\sigma$ and $\ell og\ t_f$ for 2 mol% Y_2O_3-TZP with a grain size of 0.46μm (Z2Y-Ⅰ) at 250℃ is shown in Fig.19. The relationship was linear at the applied stress more than 560MPa, but the relationship deviated from the linear one in the vicinity of 560MPa and showed the tendency corresponding to fatigue limit. The time-to-failure of Z2Y-Ⅰ obtained by the static fatigue technique was shorter than that estimated from dynamic fatigue data, and the N value was smaller than that from dynamic fatigue results.

Fig.20 shows the relationship between applied stress σ and time-to-failure t_f for 4 mol% Y_2O_3-TZP with a grain size of 1.34μm (Z4Y-Ⅱ) at 250℃. There is a linear relation between $\ell og\sigma - \ell og t_f$ and the N value obtained from the slope was 7.3. THe N value was close to N value of 8.7 obtained by dynamic fatigue technique. The average time-to-failure measured by the static fatigue technique almost agreed with that predicted

from dynamic fatigue data, too.

3.4 Fracture Surface

3.4.1 Fracture surface after dynamic fatigue test[10)-12) 15)]

Fig.21 shows the fracture surface of 3mol%Y_2O_3-TZP(Z3Y-I) after dynamic fatigue test at room temperature. It shows a smooth region near the fracture origin followed by a rougher area being spread in a radial manner. The fracture surfaces for 2 or 4mol%Y_2O_3-TZP at room temperature were similar to those for 3mol%Y_2O_3-TZP, too. That is, the fracture surfaces of Y-TZP obtained at room teperature were similar to the typical fracture surface observed in many ceramics.[57)-60)]

Fig.22(a) and (b) show fracture surfaces after dynamic fatigue test at a stressing rate of 0.302MPa/s (crosshead speed : 0.005mm/min) at 250℃ for 3mol%Y_2O_3-TZP. A fatigue fracture surface was not observed even at the slowest stressing rate of 0.302MPa/s for the specimen with a small grain size of 0.53μm (Z3Y-I) as shown in Fig.22(a) and an enlarged mirror rigion was observed. On the other hand, a fatigue fracture surface was observed at the slowest stressing rate of 0.302MPa/s for the specimen with a large grain size of 1.06μm (Z3Y-II) as shown in Fig.20(b) but was not observed at a higher stressing rate of 3.02MPa/s.

Fig.23 show a fracture surface after dynamic fatigue test at stressing rates of 3.02MPa/s (crosshead speed : 0.05 mm/min) and 0.302MPa/s (crosshead speed : 0.005mm/min) for 2mol%Y_2O_3-TZP with a grain size of 1.33μm (Z2Y-II). At the stressing rate of 30.2MPa/s (crosshead speed : 0.5mm/min), a mirror region almost disappeared but a fatigue fracture surface was obscure. At a slow stressing rate of 3.02MPa/s, a fatigue fracture surface was remarkably observed on the tension side of specimens as shown in Fig.23(a). At the lowest stressing rate of 0.302MPa/s, a fatigue fracture surface occupied more than two-third of the fracture surface as shown in Fig.23(b).

Fig.24 shows a fracture surface after dynamic fatigue test at 250℃ for 2mol%Y_2O_3-TZP with a grain size of 0.46μm(Z2Y-I). A slight mirror region was observed around fracture origin at a stressing rate of 30.2MPa/s (crosshead speed : 0.5mm/min) as shown in Fig.24(a). The mirror region disappeared at a stressing rate of 3.02MPa/s(crosshead speed : 0.05mm/min) but a fatigue fracture surface was obscure. A remarkable fatigue fracture surface was observed at the lowest stressing rate of 0.302MPa/s (crosshead speed : 0.005mm/min) as shown in Fig.24(b). However, the boundary between a fatigue fracture surface and a catastrophic fracture surface was indistinct. the reason why the boundary is indistinct is supposed to be that the difference between unevennes of both the fatigue fracture surface and the catastrophic fracture surface was negligible because the grain size is small and the fracture pattern of grains on both fracture surfaces is the same intergranular fracture.

Fig.25 shows a fracture surface after dynamic fatigue test at the slowest stressing rate of 0.302MPa/s (crosshead speed : 0.005mm/min) at 250℃ for 4 mol%Y_2O_3-TZP. A mirror region was observed for 4mol%Y_2O_3-TZP with a grain size of 0.62μm(Z4Y-Ic) even at the slowest stressig rate as shown in

Fig.25(a). However, the mirror region disappeared at the slowest stressing rate of 0.302MPa/s in the case of 4mol%Y_2O_3-TZP with a grain size of 1.34μm (Z4Y-II) but a fatigue fracture surface was obscure. A fatigue fracture surface was obviously observed at the lowest stressing rate of 0.302MPa/s (crosshead speed : 0.005mm/min) for 4mol%Y_2O_3-TZP with a grain size of 2.08μm(Z4Y-III)[11]

In summerry of the fracture surface after dynamic fatigue test, that at room temperature show a mirror region near the fracture origin and the mirror region was surrounded by a huckle region being spread in a radial manner as already described. It is estimated that the stressing rates for the mirror region to disappear and for the fatigue fracture surface to appear were 3.02MPa/s for grain size group of 0.5μm(Z2Y-I) and 30.2MPa/s for 1μm group(Z2Y-II) in the case of 2mol%Y_2O_3-TZP. In the case of 3mol%Y_2O_3-TZP, a fatigue fracture surface was not observed even at the lowest stressing rate of 0.302MPa/s for grain size group of 0.5μm(Z3Y-I), but began to appear at a stressing rate below 3.02MPa/s for grain size group of 1μm(Z3Y-II). In the case of 4mol%Y_2O_3-TZP, a fatigue fracture surface was not observed even at the lowest stressing rate of 0.302MPa/s for grain size group of 0.5μm(Z4Y-I), but began to appear at a stressing rate of 0.302MPa/s for grain size group of 1μm(Z4Y-II)

3.4.2 Fracture surface after static fatigue test[10) 13) 15)]

Fig.26 shows a fracture surface after static fatigue test at 250℃ for 3mol%Y_2O_3-TZP with a grain size of 1.06μm(Z3Y-II). A fatigue fracture surface was observed on the tension side in a bending specimen above time-to-failure of 1 hour. An area of fatigue fracture surface increased with increasing time-to-failure.

Fig.27 shows a fracture surface after static fatigue test at 250℃ for 2mol%Y_2O_3-TZP with a grain size of 0.46μm(Z2Y-I). A mirror region was observed around fracture origin for the specimen which time-to-failure was short as shown in Fig.27(a). On the other hand, a fatigue fracture surface was observed for the specimen which time-to-failur was longer as shown in Fig.27(b) and (c). However, the boundary between the fatigue fracture surface and the catastrophic fracture surface was obscure in a similar manner as FIg.24(b).

Fig.28 shows a fracture surface after static fatigue test at 250℃ for 4mol%Y_2O_3-TZP with the grain size of 1.34μm(Z4Y-II). The fracture surface was similar to that after dynamic fatigue test and the distinct fatigue fracture surface was not observed.

3.5 Comparison between time-to-failure measured by static fatigue technique and that predicted from dynamic fatigue data.

As a fatigue fracture surface in Fig.26 is distinct, fracture toughness of 3mol%Y_2O_3-TZP with grain size of 1.06μm at 250℃ may be estimated by taking the fatigue fracture surface as precrack in catastriphic fracture. The estimated fracture toughness was shown in Fig.29 as a function of the area of a fatigue fracture surface or a catastophic fracture surface. The

larger the time-to-failure, namely the area of fatigue fracture surface became, the larger the estimated fracture toughness K_{IC} became.

Fig.30 shows a schematic figure relating to a fracture surface containing both the fatigue fracture surface and the catastrophic fracture surface. Compression stress $\Delta\sigma$ is developed at the tip of crack by the t→m transformation. In this case, fracture stress σ_f was expressed by following equation.

$$\sigma_f = \sigma_0 + \Delta\sigma \qquad (11)$$

where σ_0 is fracture stress of matrix in the case that stress induced phase transformation is not occured. Taking crack length immediately before catastrophic fracture as "a", equations $K_{IC} = Y\sigma\sqrt{a}$ and $K_{IC}^0 = Y\sigma_0\sqrt{a}$ were derived. Substituting these equations into Eq.(11), fracture toughness K_{IC} can be written as following equation.

$$K_{IC} = K_{IC}^0 + k\sqrt{a}\ \Delta\sigma \qquad (12)$$

Assuming that $\Delta\sigma$ is constant, The larger the length of crack, namely, the larger the area of fatigue fracture is, the larger the fracture toughness is. The larger the fatigue fracture surface becomes, the larger the ratio of the contribution of $\Delta\sigma$ to fracture stress becomes. As $\Delta\sigma$ acts as the resistance to the crack extension, the effect of the resistance to the crack extension is considered to increase with increasing the area of a fatigue fracture surface.

The life time measured by static fatigue technique was longer than that predicted from dynamic fatigue technique for Z3Y-Ⅱ as shown in Fig.18. On the other hand, difference between measured life time and predicted one is small for Z4Y-Ⅱ as shown in Fig.20. The reason why the relationship between measured life time and predicted one is different in the case of Z3Y-Ⅱ and Z4Y-Ⅱ is considered to be responsible for the difference in the amount of t→m transformation between their specimens. It is estimated from Eqs.(11) and (12) that the life time measured by static fatigue technique become longer than that predicted from dynamic fatigue data because the contribution of the compression stress to fracture stress and fracture toughness in static fatigue test is larger than that in dynamic fatigue test, that is, because the area of fatigue fracture surface in static fatigue is larger than that in dynamic fatigue as shown in Fig.29.

The larger the amount of t→m transformation becomes, the larger the contribution of the compression stress at tip of crack becomes. The volume percent of t→m transformation for Z3Y-Ⅱ was 45.6%, while that for Z4Y-Ⅱ decreased up to 16.2%. That is, it is estimated that the compression stress at tip of crack for Z4Y-Ⅱ become smaller than that for Z3Y-Ⅱ. As the contribution of phase transformation to fatigue behavior in Z4Y-Ⅱ becomes small, the contribution of stress corrosion being principal reason for fatigue in many oxide ceramics such as alumina may become more remarkable. This is probably the reason why the time-to-failure measured by static fatigue technique become near to the value estimated from the data of dynamic fatigue in the case of Z4Y-Ⅱ. while, it is estimated that the contribution of $\Delta\sigma$ in Eqs.11 and 12 for Z3Y-Ⅱ becomes large as the amount of t→m transformation is large. This is probably the reason why the time-to-failure measured by static fatigue technique become larger than

that predicted from dynamic fatigue data as the area of fatigue fracture surface in static fatigue become larger than that in dynamic fatigue for Z3Y-Ⅱ. There is the possibility that the contribution of $\Delta\sigma$ in fatigue behavior of Z2Y-Ⅰ become larger than that in Z3Y-Ⅱ as the amount of phase transformation in Z2Y-Ⅰ is 51.5%. On the other hand, it is known that Z2Y-Ⅰ exhibits the degradation of strength by long period of thermal aging in air at 250℃ even if external stress do not applied. That is, in the case of the degradation of strength measured by long period of applied stress such as static fatigue test for Z2Y-Ⅰ, the degradation of strength by thermal aging is superposed on that by fatigue. The large contribution of thermal aging for degradation of strength is probably the reason why the time-to-failure predicted from dynamic fatigue data became shorter than that obtained by static fatigue test in the case of Z2Y-Ⅰ.

3.6 Effect of water to fatigue behavior[14)]

Figs 31 and 32 show the results obtained by dynamic fatigue technique for Z3Y-Ⅰb(grain size : 0.5μm) and Z3Y-Ⅱb(grain size : 1.12μm) in water at room teperature(20℃), and in air and water at 95℃. There were linear relationships between $\ell og\sigma_f$ and $\ell og\dot{\sigma}$ in water at room temperature and in air at 95℃ for Z3Y-Ⅰb. The N values obtained from their slops were 47.8 in water at room teperature and 46.4 in air at 95℃. These N values are similar to that of Z3Y-Ⅰ at room temperature shown in Fig.5. On the other hand, the relationship between $\ell og\sigma_f$ and $\ell og\dot{\sigma}$ in water at 95℃ at the stressing rate below 3.27MPa/s (crosshead speed : 0.5mm/min) was similar to the relationship in air at 95℃, too. However, the fracture stress at a stressing rate above 3.27MPa/s showed a constant value even if stressing rate increased.

There is a linear relationship between $\ell og\sigma_f$ and $\ell og\dot{\sigma}$ in water at room temperature for Z3Y-Ⅱb, too. The N value obtained from the slop was 47.5 being similar to that for Z3Y-Ⅰb. However, relationships in air and water at 95℃ were different to those for Z3Y-Ⅰb. A relationship between $\ell og\sigma_f$ and $\ell og\dot{\sigma}$ below a stressing rate of 30.2MPa/s in air at 95℃ was similar to the relationship in water at room temperature but fracture stress at a stressing rate above 30.2MPa/s became constant. On the other hand, the fracture stress in water at 95℃ showed a constant value in the range of stressing rates measured in this study. The behavior showing the constant value in water became more remarkable than in air and the constant fracture stress σ_{max} in water had lower value than that in air. It is estimated that the relationship between $\ell og\sigma_f$ and $\ell og\dot{\sigma}$ in water at 95℃ in the case of Z3Y-Ⅱ became parallel to the horizontal axis, because the value correspond to $\dot{\sigma}_s$ in Fig.33 was below 0.327MPa/s(crosshead speed: 0.005mm/min).

3.7 Degradation of strength in Y-TZP[10)-15)]

The summary of the results obtained in this study on the fatigue behavior of TZP containing 3mol%Y_2O_3 (Y-TZP) are as follows.

(1) At room remperature, there were linear relationships between $\ell og\sigma_f$

and $\ell og\dot{\sigma}$ for both grain size group of 0.5 and 1μm in air and in water. The N values obtained were 41.0 to 53.6 indicating slight fatigue.

(2) For grain size group of 0.5μm, the relationship between $\ell og\sigma_f$ and and $\ell og\dot{\sigma}$ in air at 95℃ was linear at the whole range of stressing rate. The N value obtained was 46.4 indicating slight fatigue. On the other hand, the relationship in water at 95℃ was linear at the stressing rate below 3.27MPa/s, too. However, the relationship above 3.27MPa/s became parallel to the horizontal axis.

(3) For grain size group of 1μm in air at 95℃, the relationship between $\ell og\sigma_f$ and $\ell og\dot{\sigma}$ was linear at the stressing rate below 3.27MPa/s. However, fracture stress at the stressing rate above 32.7MPa/s became constant even if the stressing rate increased. On the other hand, in water at 95℃, the fracture stress was constant in the whole range of stressing rate. The fracture stress showing constant value in water at 95℃ became lower than that in air.

(4) In air at 250℃, there were linear relationships between $\ell og\sigma_f$ and $\ell og\dot{\sigma}$ for grain size group of 0.5μm in the whole range of stressing rate. The N values obtained were 50.5, indicating slight fatigue. On the other hand, the relationship for grain size group of 1μm was linear below the stressing rate of 30.2MPa/s. However, fracture stress became constant at a stressing rate above 30.2MPa/s even if stressing rate increased. The N value obtained was 10.2 indicating remarkable fatigue.

Fig.33 is a schematic relationship between $\ell og\sigma_f$ and $\ell og\dot{\sigma}$ designed to represent the summary of (1) through (4). This relationship is divided into two types. The first is a linear relationship for all specimens at room temperature or for the specimen with small grain size in the case of temperature above 95℃. The second is the phenomena which fracture stress become constant above a certain stressing rate, namely the phenomena regarded as innert strength. As already described, this phenomena is affected by Y_2O_3 contents, grain sizes or atmosphere. In this study, this phenomena is called the maximum attained strength. This second relationship is characterized by the maximum attained strength σ_{max}, the stressing rate $\dot{\sigma}_s$ at a point where the fracture stress begins to decrease from the maximum attained strength σ_{max} with decreasing stressing rate, and the relationship between $\ell og\sigma_f$ and $\ell og\dot{\sigma}$ at stressing rate below $\dot{\sigma}_s$.

We consided on the basis of above described results that the degradation of strength in Y-TZP should be classified into two mechanism, that is, degradation of strength in connection with the formation of monoclinic zirconia from tetragonal zirconia by the reaction with water or moisture in atmosphere at above 90℃ (abbreviated to degradation of strength by thermal aging. This degradation is not affected by external applied stress) and degradation of strength in connection with t→m transformation accelerated by external applied stress(that is, fatigue). We suppose that the phenomena showing a constant fracture stress at the stressing rate above $\dot{\sigma}_s$ appearing in the relationship between $\ell og\sigma_f$ and $\ell og\dot{\sigma}$ relate to chemical reaction of tetragonal zirconia with water or moisture in atmosphare. The part relating to fatigue behavior in the $\ell og\sigma_f - \ell og\dot{\sigma}$ relationship is the slope below $\dot{\sigma}_s$.

Tetragonal zirconia on the surface of the specimen change to monoclinic zirconia by the reaction with water or moisture in atmosphare resulting in reduced strength.[61)-67)] Although fracture stress σ_f increase with increasing a stressing rate $\dot{\sigma}$, it does not increase beyond the fracture stress limited by the chemical reaction of tetragonal zirconia with water or moisture in atmosphere. The strength limited by the chemical reaction with water or moisture in atmosphere correspond to the maximum attained strength σ_{max} and it is greatly affected by grain size and vapor pressure P_{H_2O}. The higher the P_{H_2O} is, the more the σ_{max} is. The effect of P_{H_2O} become more remarkable in the specimen with larger grain size.

It is generally known that fatigue of glass and oxide ceramics is greatly affected by water or moisture in atmosphere. The water is consided to affect fatigue behavior by following mechanism : When a crack grows by external stress applied to glass or ceramics, water in atmosphere facilitates the breaking of bond and enhances the crack growth.[68)-70)] On the other hand, high strength and toughness in TZP relate to the transformation of tetragonal zirconia into monoclinic zirconia within the process zone produced ahead of the crack tip during crack growth.[71)] As already described, fatigue of TZP relates closely to this phase transformation. For water to affect fatigue, constituent elements of water such as O^{2-} or OH^- need to diffuse in the process zone. The measurement of electrical conductivity suggests that diffusion of the elements such as O^{2-} or OH^- is easy at 250℃ but difficult below 100℃.[72)-75)]

It is apparent from Figs.16 and 17 that the relationship of $\log\sigma_f$ - $\log\dot{\sigma}$ for Z3Y-Ⅰb and Z3Y-Ⅱb is in the region of flaw limited stength at room temperature. Although there is no data accumulated at 95℃, it can be supposed from the correspondence with data at room temperature that Z3Y-Ⅰb and Z3Y-Ⅱb is in the region of flaw limited stength at 95℃ as well. On the other hand, It is considered that Z3Y-Ⅰ at 250℃ is in the region of flaw limited stength, while Z3Y-Ⅱ at 250℃ is in the region of transformation limited strength. At room temperature, fatigue is slight in the air because both Z3Y-Ⅰb and Z3Y-Ⅱb are in the region of flaw limited stength. Fatigue of these specimens is slight in water at room temperatur as well and show a similar tendency to that in air, because the reaction of tetragonal zirconia with water can be neglected at room temperature even if their specimens are dipped into water.

Fatigue of zirconia ceramics in water is reported by Li and Pabst,[20)] and Becker.[22)] Li et al. measured the crack growth parameter N of zirconia containing 7mol%MgO and 4mol%CaO by the double torsion technique and dynamic fatigue technique, and reported the N value above 50 in water at room temperature. Becker measured the relationship between stress intensity factor K_I and crack growth velocity V for zirconia containing 7.2mol%MgO (average grain size : 60μm), and reported 121 in air and 120 in water as the N value at 22℃. However, K_I - V curve in water is shifted to higher crack growth velocity than that in air in comparison at same K_I. Depicted by the relationship in dynamic fatigue, namely, by the relationship of $\log\sigma_f$ and $\log\dot{\sigma}$, the slope of the relationship in water is similar to that in air. However, the difference between K_I - V curvees in water and in

air correspons to that the fracture stress in water reduces up to 80% of that in air in comparison at same stressing rate. Fig.34 shows fracture stress of Z3Y-I and Z3Y-II in air and water at room temperature. The fracture stress of Z3Y-I in water is about 96% of that in air and the fracture stress of Z3Y-II in water is near to that in air. That is, in the case of Y-TZP, there were not remarkable difference between fracture stresses in water and in air.

It is known that tetragonal zirconia changes to monoclinic zirconia by the reaction with water in hot water above 90℃. Therefore, we checked to what entent the degradation of strength of Z3Y-I b and Z3Y-II b reduces by dipping for 96 hours in water at 98℃. Consequently, it became apparent that the change of strength with dipping time for Z3Y-I was negligible, even after 96 hours. On the other hand, the change of strength for Z3Y-II was slightly at 24 hours and negligible above 24 hours. The monoclinic zirconia contents on specimen surfaces increased 4% for Z3Y-I b and 13% for Z3Y-II b after dipping in hot water for 96 hours. By considering that the longest dipping time in dynamic fatigue test was about 1 hour, it is estimated that the phenomena in Figs.31 and 32 resulted from that the external stress was applied. When a specimen is dipped in water at 95℃ under external stress, the reaction area is increased by the formation of crack on the specimen surface in tesion side and the growth of crack toward inside. Consequently, the reaction with water is enhanced.

The reaction of TZP with water become more remarkable in the spesimen with a larger grain size. For Z3Y-I b with a grain size of about 0.5μm, the stressing rate corresponding to σ_s in Fig.34 is 32.7MPa/s (crosshead speed :0.5mm/min). In the case of Z3Y-II b with a larger grain size of about 1μm, the reaction with water becomes more remarkable than that of Z3Y-I b. Therefore, the maximum attained strength σ_{max} becomes lower than that in the absence of water. As a result, $\dot{\sigma}_s$ of Z3Y-II b shifts to a stressing rate of 0.327MPa/s (crosshead speed : 0.005mm/min). This is probably responsible for that only the region corresponding to the maximum attained strength σ_{max} apperars.

Concerning relationship between the $\ell og\,\sigma_f$ and $\ell og\,\dot{\sigma}$ below $\dot{\sigma}_s$ for Z3Y-I b, it is estimated that there is not a great difference between the slope in water at 20℃ and that in water at 95℃. As already described, oxygen or other elements must diffuse in the process zone ahead of the crack tip in order for the water to affect fatigue behavior, but diffusion can be neglected at a temperature of about 95℃. Therefore, the effect of water on fatigue of Z3Y-I b is small, and the slope below $\dot{\sigma}_s$ may have a similar tendency between the slope in water at 20℃ and that in air at 95℃. As $\ell og\,\sigma_f - \ell og\,\dot{\sigma}$ relationship below $\dot{\sigma}_s$ for Z3Y-II with grain size of 1μm could not be measured, the effect of water to fatigue behavior in not clear, but the effect is supposed to be as small as that for Z3Y-I b.

The $\ell og\,\sigma_f - \ell og\,\dot{\sigma}$ relationship at 250℃ for Z3Y-II (grain size : 1.06μm) shows a constant value above $\dot{\sigma}_s$ corresponding to a stressing rate of 30.2 MPa/s (crosshead speed : 0.5mm/min), as described in summary(4) at the beginning of this section. Although we do not measure the relationship between $\ell og\,\sigma_f$ and $\ell og\,\dot{\sigma}$ under the change of P_{H_2O} in atmosphare, it is estimated to be due to the reaction between tetragonal zirconia and moisture

in air that the phenomena corresponding to maximum attained strength σ_{max} appears for Z3Y-Ⅱ with a large grain size. Whereas, there is a linear relationship for Z3Y-Ⅰ. The reason why σ_{max} appears on Z3Y-Ⅱ and do not on Z3Y-Ⅰ is considered to be as follows : since the vapor pressure of water in the atmosphare is lower compared with the case of dipping in water, tetragonal zirconia reacts slightly with moisture for Z3Y-Ⅰb with a small grain size, therefore, σ_{max} shifts to a larger fracture strength compared with the case of Z3Y-Ⅱ

Next, let's consider $\ell og\sigma_f - \ell og\dot{\sigma}$ relationship below $\dot{\sigma}_s$ relating to fatigue behavior. As described in summary(4) at the beginning of this section, the slope of $\ell og\sigma_f - \ell og\dot{\sigma}$ relationship for Z3Y-Ⅱ is large in air at 250℃, indicating remarkable fatigue. As described in previous section, fatigue behavior in Z3Y-Ⅱ become remarkable in the condition that water is absent because the $\sigma_f - \sqrt{h}$ relationship is in the region of transformation limited strength. On the other hand, for Z3Y-Ⅰ with a grain size of about 0.5μm, $\sigma_f - \sqrt{h}$ relationship is in thr region of flaw limited strength, so that fatigue is considered to be slight, which agree well with the experimental results. The measurement of electrical conductivity on Y-TZP suggests that the diffusion of oxygen or other elements cannot be neglected around 250℃. That is, the effect of water on fatigue through the diffusion of oxygen is considered to be possible. As there are no remarkable difference in electrical conductivity between specimens with the grain size of about 0.5μm and about 1μm, fatige for Z3Y-Ⅰ would be remarkable as well as for Z3Y-Ⅱ if fatigue behavior affected by water as described above. However, this is not shown by the experimental result. From this consideration, the reason why fatigue behavior is remarkable in air at 250℃ is considered to be that the $\sigma_f - \sqrt{h}$ relationship on Z3Y-Ⅱ is in the region of transformation limited strength.

4. CONCLUSIONS

The fatigue behavior of 2, 3 and 4 mol% Y_2O_3-TZP at room temperature and at 250℃ was studied by dynamic fatigue technique. Results obtained are as folows:

1) The relationship between stress and displacement was linear up to fracture stress indicating elastic behavior at room temperature for all speciments used in this study. The stress-displacement relationship at 250℃ for 3 and 4 mol%Y_2O_3-TZP showed the elastic behavior at the whole range of stressing rate used in this study, too. The relationship at 250℃ for 2 mol%Y_2O_3-TZP was elastic at the stressing rate above 3.02MPa/s but inelastic at the stressing rate of 0.302MPa/s.

2) The crack growth parameter N at room temperature was 63.7 to 104 for 2 mol%Y_2O_3-TZP, 41.0 to 53.6 for 3mol%Y_2O_3-TZP and 31.7 to 46.1 for 4 mol% Y_2O_3-TZP. The N value decreased with increasing Y_2O_3 contents.

3) The N value at 250℃ for Y-TZP with a grain size above 1μm was below 10 indicating remarkable fatigue.

4) The N value at 250℃ for grain size group of 0.5μm was about 50 for

3mol%Y_2O_3-TZP. If Y_2O_3 content decreased to 2 mol% or increased up to 4 mol%, the N value decreased until 22 or 32.3 to 40.9, respectively.

5) Monoclinic zirconia contents on the fracture surface after dynaminc fatigue test decreased with increasing Y_2O_3 contents for a certain grain size group and with decreasing grain size for a ceratain Y_2O_3 contents.

6) The crack growth parameter N may be arranged by using the thickness of transformation zone h as a parameter indicating amount of transformation from tetragonal zirconia to monoclinic one. The N value increased with increasing h at room temperature. The N value at 250℃ for grain size group of 0.5μm is similar to that at room temperature up to h around 0.6 μm. However, The N value decreased with increasing h value at h above 0.6μm. The N value at 250℃ for grain size group of 1μm was average of 9.2 regardless of transformation zone size h.

The fatigue behavior of 2, 3 and 4 mol%Y_2O_3-TZP at 250℃ was studied by static fatigue technique. Results obtained are as follows:

7) The crack growth parameter N for 3 mol%Y_2O_3-TZP with a grain size of 1.06μm was 10.7 near to that obtained from dynamic fatigue technique. However, the time-to-failure obtained by static fatigue technique was 4 to 6 times that predicted from dynamic fatigue data

8) The N value for 2 mol%Y_2O_3-TZP with a grain size of 0.46μm was 10.8 and became smaller than that obtained from dynamic fatigue technique. The time-to-failure obtained by static fatigue technique was shorter than that predicted from dynamic fatigue data.

9) The N value for 4 mol%Y_2O_3-TZP with a grain size of 1.34μm was 7.3 near to that obtained from dynamic fatigue technique. The time-to-failure obtained by static fatigue technique almost agreed with that predicted from dynamic fatigue data.

Fracture surface after dynamic fatigue and static fatigue tests was observed by SEM. Results obtained are as follows:

10) Fracture surfaces after dynamic fatigue test at room temperature showed a smooth region near the fracture origin followed by a rougher area being spread in a radial manner for all specimens used in this study and were similar to the typical fracture surface observed in many ceramics.

11) On the fracture surface after dynamic fatigue test at 250℃, the larger the grain size became or the lower the stressing rate became, the more remarkable the fatigue fracture surface became.

12) The remarkable fatigue fracture surface was observed on the fracture surface after static fatigue test at 250℃ for 2 or 3 mol%Y_2O_3-TZP. The longer the time-to-failure became, the larger the fatigue fracture surface became.

The fatigue behavior of 3mol%Y_2O_3-TZP in water at room temperarure and 95℃ was studied by dynamic fatigue technique. Results obtained are as follows:

13) fatigue behavior in water at room temperature was similar to that in air at room temperature and the fatigue was slight

14) For the grain size group of 0.5μm, the $\ell og\sigma_f - \ell og\dot{\sigma}$ relationship in air at 95℃ became linear and was similar to that at room temperature. the $\ell og\sigma_f - \ell og\dot{\sigma}$ relationship in water at 95℃ became similar to that in air at 95℃ at stressing rate below 32.7MPa/s, too. However, the

relationship showed a constant value at the stressing rate above 32.7MPa/s.

15) For the grain size group of 1μm, the $\log\sigma_f$ - $\log\dot{\sigma}$ relationship in air at 95℃ was similar to that at room temperature at stressing rate below 32.7MPa/s. The relationship in water at 95℃ showed the constant value at the stressing rate above 0.327MPa/s to be slowest stressing rate in this study.

16) The phenomena that fracture stress became constant even if stressing rate increased is remarkable in large grain size and in water rather than air.

References

1) Advanced in Ceramics, Vol.3, Science and Technology of Zirconia, Edited by A.H.Heuer and L.W.Hobbs, The Amer.Ceram.Soc.Inc.(1981).
2) Advanced in Ceramics, Vol.12, Science and Technology of Zirconia II, Edited by N.Claussen, M.Ruhle and A.H.Heuer, The Amer.Ceram.Soc.Inc. (1984)
3) Advanced in Ceramics, Vol.24A and 24B, Science and Technology of Zirconia III, Edited by S.Somiya, N.Yamamoto and H.Yanagida, The Amer. Ceram.Soc.Inc.(1988).
4) R,J,Charles : "Static fatigue of glass I and II" J.Appl.Phys. 29, 1549-1560(1958).
5) R,J,Charles : "Dynamic fatigue of glass" J.Appl.Phys. 29, 1657-1662 (1958).
6) R.E.Mould and R.D.Southwick : "Strength and static fatigue of abraded glass under controlled ambient codition : II, Effect of various abration and the universal fatigue curve" J.Amer.Ceram.Soc., 42, 582-592(1959).
7) J.E.Burke, R.H.Doremus, W.B.Hillig and A.M.Turkalo : "Static fatigue in glasses and alumina" p.435-444, in Ceramics in severe environments, Materials Science Research Vol.5, Edited by W.W,Kriegel and H.Palmour III, Plenum Press(1971).
8) S.M.Wiederhorn : "Subcritical Crack Growth in Ceramics", pp.613-646 in Fracture Mechanics of Ceramics, Vol.2 , Microstructure, Materials, and Applications, Edited by R.C.Bradt,D.P.H.Hasselman and F.F.Lange, Plenum Press, New York(1974).
9) K.Tsukuma and M.Shimada : "Thermal stability of Y_2O_3-partially stabilized zirconia(Y-PSZ) and Y-PSZ/Al_2O_3 composites" J.Ma,ter.Sci. Letters, 4, 857-861(1985).
10) M.Ashizuka, H.Kiyohara, E.Ishida, M.Kuwabara and T.Tsukidate : "Fatigue behavior of Y_2O_3-partially stabilized zirconia" Yogyo-kyokai-shi (J.Ceram.Soc.Japan), 94, 432-439(1986).
11) M.Ashizuka, H.Kiyohara, M.Gondo and Y.Kubota : "Fatigue behavior of 2 and 4 mol%Y_2O_3-containing tetragonal zirconia polycrystals(Y-TZP)" Yogyo-Kyokai-Shi(J.Ceram.Soc.Japan), 95, 387-393(1987). Journal Ceramic Society of Japan, International Edition, 95, 348-353(1987).
12) M.Asizuka, H.Kiyohara, T.Okuno and Y.Kubota : "Fatigue behavior of tetragonal zirconia polycrystals(Y-TZP) containing 2 and 4 mol%Y_2O_3 (Part 2)" Journal of The Ceramic Society of Japan, 96, 749-754(1988).

Journal Ceramic Society of Japan, International Edition, 96, 731-736 (1988).

13) M.Ashizuka, H.Kiyohara, T.Okuno and Y.Kubota : "Static fatigue of 2mol% Y_2O_3-containing tetragonal zirconia polycrystala at 250℃ " Journal of The Ceramic Society of Japan , 96, 820-824(1988). Journal Ceramic Society of Japan, International Edition, 96, 798-802(1988).

14) M.Ashizuka and Y.Kubota : : Journal of The Ceramic Society of Japan "Effect of water to fatigue behavior of yttria-containing tetragonal zirconia polycrystals" Journal of The Ceramic Society of Japan, 96, 1186-1191(1988). Journal Ceramic Society of Japan, International Edition, 96, 1157-1161(1988).

15) M.Ashizuka, T.Honda and Y.Kubota : "Fatigue behavior of tetragonal zirconia polycrystals containing 4mol%Y_2O_3" Journal of The Ceramic Society of Japan, 99,(1991),(in press). Journal Ceramic Society of Japan, International Edition, 99, (1991),(in press).

16) S.M.Wiederhorn : "Influence of water vapor on crack propagation in soda-lime glass" , J.Amer.Ceram.Soc., 50, 407-414(1967)

17) S.M.Wiederhorn and L.H.Bolz : "Stress corrosion and static fatigue of glass" , J.Amer.Ceram.Soc., 53, 543-548(1970).

18) S.M.Wiederhorn and H.Johnson : "Effect of electrolyte pH on crack propagation in glass" , J.Amer.Ceram.Soc., 56, 192-197(1973).

19) A.G.Evans : "Method for evaluation the time-dependent failure characteristics of brittle materials and its application to polycrystalline alumina" J.Mater. Sci., 7, 1137-1146(1972).

20) Li-Shing Li and R.F.Pabst : "Subcritical crack growth in partially stabilized zirconia(PSZ)" J.Mater.Sci., 15, 2861-2866(1980).

21) P.F.Becker : "Slow crack growth behavior in transformation-toughened Al_2O_3-ZrO_2(Y_2O_3) ceramics" , J.Amer.Ceram.Soc., 66, 485-488(1983).

22) P.F.Becker : "Subcritical crack growth in partially stabilized ZrO_2(MgO)" J.Mater.Sci., 21, 297-300(1986).

23) R.H.Dayskardt, W.Yu, and R.O.Ritchie : "Fatigue crack propagation in transformation-toughened zirconia ceramics" J.Amer.Ceram.Soc., 70, C-248-C-252(1987).

24) R.H.Dauskardt, D.B.Marshall and R.O.Ritchie "Cyclic fatigue-crack propagation in magnesia-partially-stabillized zirconia ceramics" J.Amer.Ceram.Soc., 73, p.893-903(1990).

25) O.Kamigaito : "Mechanicai properties of ceramics, Part.23" Bulletin of Ceramic Society of Japan, 12, 1040-1047(1977).

26) A.G.Evans and S.M.Wiederhorn : "Proof of testing of ceramic materials —an analytical basis for failure prediction" Inter.J.Fracture 10, 379 -392(1974).

27) J.E.Ritter : "Engineering design and fatigue failure of brittle materials" p.667-686 in Fracture Mechanics of Ceramics, Vol.4, Edited by R.C.Bradt, D.P.H.Hasselman and F.F.Lange, Plenum Press(1978).

28) J.E.Ritter and J.A.Meisel : "Strength and failure prediction for glass and ceramics" , J.Amer.Ceram.Soc., 59, 478-481(1976).

29) J.E.Ritter and J.N.Humenik : "Static and dynamic fatigue of polycrystalline alumina" J.Mater.Sci., 14, 626-632(1979).

30) A.G.Evans : "Slow crack growth in brittle materials under dynamic

loading condition" Inter.J.Fracture, 10, 251-259(1974).
31) A.G.Evans and H.Johnson : "The Fracture stress and its dependence on slow crack growth" J.Mater.Sci., 10, 214-222(1975).
32) H.Toraya, M.Yoshimura and S.Somiya : "Calibration curve for quantitative analysis of the monoclinic-tetragonal ZrO_2 system by X-ray diffraction" J.Amer. Ceram.Soc., 67, C-119-C-121(1984).
33) H.Toraya, M.Yoshimura and S.Somiya : "Quantitative analysis of monoclinic-tetragonal ZrO_2 system by X-ray diffraction" p.53-59 in Zirconia Ceramics, Vol.2, Edited by Somiya and M.Yoshimura. Uchida Rokakuho Publishing Co.,(1986).
34) T.Kosmac, R.Wagner and N.Claussen : "X-ray determination of transformation depths in ceramica containing tetragonal ZrO_2" , J.Amer.Ceram.Soc., 64, C-72-C-73(1981).
35) R.A.Miller, J.L.Smialek and R.G.Garlick,"Phase stability in plasma-sprayed partially stabilized zirconia-yttria ", p.241-248 in Advances in Ceramics, Vol.12, Science and Technology of Zirconia II Ed. by N.Claussen,M.Ruhle and A.H.Heuer, The Amer.Ceram.Soc.Inc.(1984).
36) J.Lankford : "Deformation and fracture of yttria-stabilized zirconia single crystals" J.Mater.Sci., 21, 1981-1989(1986).
37) J.Lankford : "Plastic deformation of partially stabilized zirconia" J.Amer.Ceram.Soc., 66, C-212-C-213(1983).
38) M.V.Swain, "R curve behavior magnesia partially stabilized zirconia and its significance to thermal shock" p.355-370 in Fracture Mechanics of Ceramics, Vol.6, Edited by R.C.Bradt,A.G. Evans,D.P.H.Hasselman and F.F.Lange, Plenum, New York (1983).
39) M.V.Swain : "Inelastic deformation of MgO-PSZ and its significance for strength-toughness relationship of zirconia toughened ceramics" , Acta Met., 33, 2083-2091(1985).
40) T.B.Troczynski and P.S.Nicholson : "Resistance to fracture of a partially stabilized zirconia/β-alumina composite" J.Amer.Ceram.soc., 68, C-277-C-279(1985).
41) K.Tsukuma and M.Shimada : "Strength, fracture toughness and vickers hardness of CeO_2-stabilized tetragonal ZrO_2 polycrystals(Ce-TZP)" J.Mater.Sci., 20, 1178-1184(1985).
42) R.H.J.Hannink and M.V.Swain : "A mode of deformation in partially stabilized zirconia" J.Mater.Sci., 16, 1428-1431(1981).
43) H.C.Chandan, R.C.Bradt and G.E.Rindone : "Dynamic fatigue of float glass" J.Amer.Ceram.Soc., 61, 207-210(1978).
44) K.K.Smith and M.B.Magida : "Dynamic fatigue of a machinable glass-ceramic" J.Am.Ceram.Soc., 66, 500-505(1983).
45) Y.Matsuo, S.Kimura, E.Yasuda and T.Inukai : "Time dependent strength distribution of brittle materials expressed by Weibull's bi-modal function" Yogyo-Kyokai-Shi(J.Ceram.Soc.Japan), 92, 274-280(1984).
46) H.G.Scott : "Phase relationships in the zirconia-yttria system" J.Mater.Sci., 10, 1527-35(1975).
47) A.H.Heuer, N.Claussen, W.M.Kriven and M.Ruhle : "Stability of tetragonal ZrO_2 particles in ceramic matrices" , J.Amer.Ceram.Soc., 65, 642-50(1982).
48) M.Ruhle and A.H.Heuer : "Phase transformation in ZrO_2-containing

ceramics Ⅱ, The martensitic reaction in t-ZrO_2", p.14～32 in Advances in Ceramics, Vol.12, Science and Technology of Zirconia Ⅱ Ed. by N.Claussen, M.Ruhle and A.H.Heuer, The Amer. Ceram. Soc. Inc.(1984).

49) A.H.Heuer and M.Ruhle : "On the nucleation of the martensitic transformation in zirconia(ZrO_2)" Acta Met., 33, 2101-2112 (1985).

50) H.Schubert : " Investigation on the stability of yttria stabilized tetragonal zirconia(Y-TZP) " p.65-81, Zirconia Ceramics, 7, Edited by S.Somiya and M.Yoshimura, Uchida Rokakuho Publishing Co.,(1986).

51) J.Burke : "The kinetics of phase transformation in metals" Pergamon Press(1965)

52) F.F.Lange : "Transformation toughening Part 1 : Size effects associated with the thermodynamics of constrained transformations" J.Mater.Sci.,17, 225-234(1982).

53) S.Schmauder and H.Schubert : "Significance of internal stresses for the martensitic transformation in yttria-stabilized tertragonal zirconia polycrystals during degradation" J.Amer.Ceram.Soc., 69, 534-540 (1986).

54) H.Schubert : "Anisotropic thermal expansion coefficients of Y_2O_3-stabilized tetragonal zirconia" J.Amer.Ceram.Soc., 69, 270-271(1986).

55) M.V.Swain : "Strength-toughness relationships for transformation toughened ceramics " p.151-162 in Fracture Mechanics of Ceramics Vol.8, Edited by R.C.Bradt, A.G.Evans, D.P.H.Hasselman and F.F.Lange, Plenum Press(1986).

56) M.V.Swain and L.R.F.Rose : "Strength limitation of transformation-toughened zirconia alloys" J.Amer.Ceram.Soc., 69, 511-518(1986).

57) J.J.Mecholsky, S.W.Freiman and R.W.Rice : "Fracture surface analysis of ceramics " J.Mater.Sci., 11, 1310-1319(1976).

58) J.J.Mecholsky, A.C.Gonzalez and S.W.Freiman : "Fractographic analysis of delay failure in soda-lime-glass" J.Amer.Ceram.Soc., 62, 577-580 (1979).

59) J.J.Mecholsky and S.W.Freiman, "Determination of fracture mechanics parameters through fractographic analysis of ceramics" p.136-150 in Fracture Mechanics Applied to Brittle Materials, ASTM STP 678, Edited by S.W.Freiman, American Society for Testing and Materials(1979).

60) R.W.Rice, S.W.Freiman, J.J.Mecholsky, R.Ruh and Y.Hanada : "Fractography of Si_3N_4 and SiC " p.669-687 in Ceramics for High Performance Application-Ⅱ, Edited by J.J.Burke, E.N.Lenoe and R.N.Katz, Brook Hill Pub. (1978).

61) T.Sato, S.Ohtaki and M.Shimada "Transformation of yttria partially stabilized zirconia by low temperature annealing in air" J.Mater.Sci., 20, 1466-1470(1985).

62) T.Sato and M.Shimada : "Transformation of yttria-doped tetragonal ZrO_2 polycrystals by annealing in water" J.Amer.Ceram.Soc., 68, 356-59(1985).

63) T.Sato and M.Shimada : "Control of the tetragonal-to-monoclinic phase transformation of yttria partially stabilized zirconia in hot water" J.Mater.Sci., 20, 3988-3992(1985).

64) F.F.Lange, G.L.Dunlop and B.I.Davis : "Degradation during aging of transformation-toughened ZrO_2-Y_2O_3 Materials at 250℃" J.Amer.Ceram. Soc., 69, 237-240(1986).

65) T.Sato, T.Endo and M.Shimada : "Improvement of the thermal stability of Y-TZP" p.47-61 in Zirconia Ceramics, Vol.9, Edited by S.Somiya and M.Yoshimura, Uchida Rokakuho Publishing Co.,(1987).
66) H.Saka, K.Kuroda, S.Iio, M.Watanabe, T.Imura, : "Effect of environmental gas on the tetragonal to monoclinic transformation in Y_2O_3-doped tetragonal ZrO_2 polycrystals and its nature" p.63-70 in Zirconia Ceramics, Vol.8, Edited by S.Somiya and M.Yoshimura, Uchida Rokakuho Publishing Co.,(1986).
67) T.Shigematsu and N.Nakanishi : "Effect of water on the phase transition of tetragonal zirconia with yttria powder during the low temperature aging" p.63-71 in Zirconia Ceramics, Vol.9, Edited by S.Somiya and M.Yoshimura, Uchida Rokakuho Publishing Co.,(1987).
68) M.Yosimura, T.Noma and K.Kawabata and S.Somiya : "The role of H_2O on the degradation process of Y-TZP" p.73-79 in Zirconia Ceramics, Vol.9, Edited by S.Somiya and M.Yoshimura, Uchida Rokakuho Publishing Co.,(1987).
69) M.Yoshimura, T.Noma, K.Kawabata and S.Somiya : "The effects of high-temperature- and high-pressure-water on the low temperature degradation behavior of Y-TZP" ,Journal of The Ceramic Society of Japan, 96, 265-270(1988).
70) S.W.Freiman : "Effect of alcohols on crack propagation in glass" J.Amer.Ceram.Soc., 57, p.350-353(1974)
71) S.W.Freiman, : "Fracture mechanics of glass" p.21-78 in Glass : Science and Technology, Vol.5, Edited by D.R.Uhlmann and N.J.Kreidl, Academic Press(1980).
72) H.Abe, Bulletin of The Ceramic Society of Japan, 17, 940-950(1982).
73) R.M.McMeeking and A.G.Evans : "Mechanics of transformation-toughening in brittle materials" , J.Amer.Ceram.Soc., 65, 242-246(1982).
74) N.Bonanos, R.K.Slotwinski, B.C.H.Steele, E.P.Butler : "High ionic conductivity in polycrystalline tetragonal Y_2O_3-ZrO_2" J.Mater.Sci. Letters, 3, 245-248(1984).
75) M.Kuwabara, T.Murakami, A.Ashizuka, K.Kubota and T.Tsukidate : "Electrical conductivity of yttria partially stabilized zirconia ceramics" J.Mater.Sci.Letters, 4, 467-471(1984).
76) S.P.S.Badwal and M.V.Swain : " ZrO_2-Y_2O_3 : Electrical conductivity of some fully and partially stabilized single grain" , J.Mater.Sci. Letters, 4, 487-489(1985).
77) N.Bonanos and E.P.Butler "Ionic conductivity of monoclinic and tetragonal yttria-zirconia single crystals" J.Mater.Sci., 4, p.561-564 (1985).

Table 1 N value and monoclinic zirconia contents on the fracture surface of Y_2O_3-containing tetragonal zirconia polycrystals.

Specimen	Y_2O_3 (mol%)	Density (g/cm³)	Grain size (μm)	Tet.★ (%)	N value R.T.	N value 250℃	Mono.(%)★ R.T.	Mono.(%)★ 250℃
Z2Y-I	2	6.01	0.46 ±0.07	98.0	104	21.9	59.9	51.5
Z2Y-II		5.96	1.33 ±0.14	97.8	67.3	8.7	74.5	77.8
Z3Y-I	3	6.02	0.53 ±0.05	71.0	53.6	50.5	21.9	28.2
Z3Y-I b		6.02	0.50 ±0.07	-	47.8★★	-	-	-
Z3Y-II		6.01	1.06 ±0.19	70.0	41.0	10.2	42.3	45.6
Z3Y-II b		5.99	1.12 ±0.12	-	47.5★★	-	-	-
Z4Y-I a	4	5.97	0.47 ±0.07	55.2	31.7	-	0	-
Z4Y-I b		6.06	0.56 ±0.04	54.3	-	32.3	-	0
Z4Y-I c		5.96	0.62 ±0.10	55.0	32.6	40.9	2.8	3.9
Z4Y-II		5.91	1.34 ±0.30	56.4	46.1	8.7	14.1	16.2
Z4Y-III		5.59	2.08 ±0.40	53.9	45.3	4.7	29.5	30.3

R.T. : Room temperature(20°～30℃).

★ Mono.(%) and Tet.(%) : Volume percent of monoclinic and tetragonal zirconia, respectively.

★★ N value in H_2O

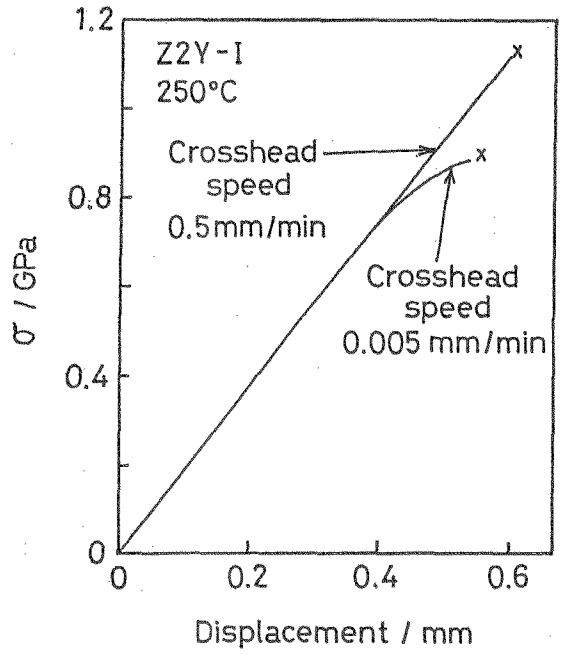

Fig.1. Stress-displacement curves of 2 mol% Y_2O_3 containing tetragonal zirconia polycrystals(Z2Y-I) at 250℃.

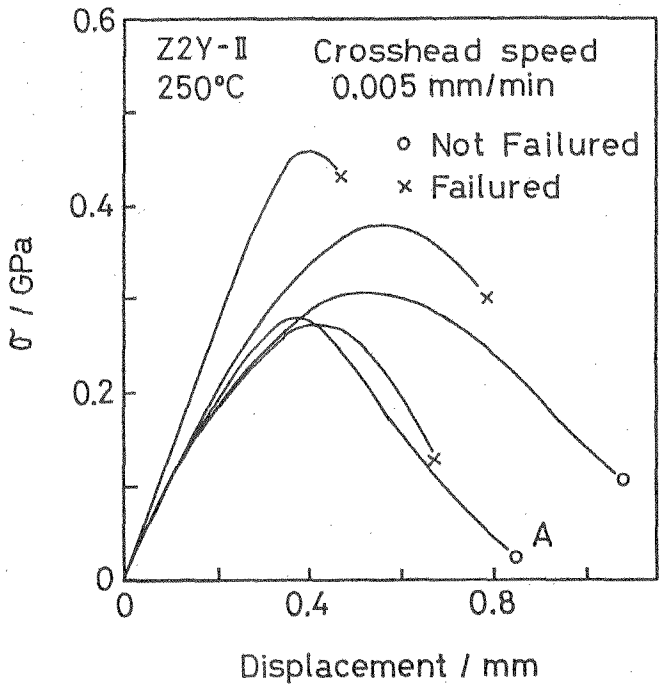

Fig.2. Stress-displacement curves of 2 mol% Y_2O_3 containing tetragonal zirconia polycrystals(Z2Y-II) at 250℃.

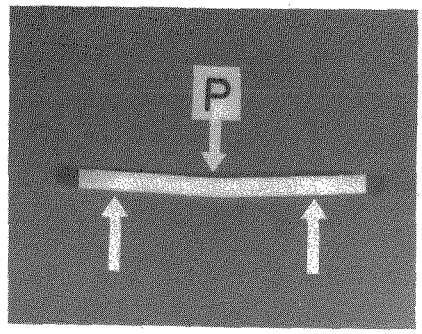

Fig.3 Potograph is specimen configuration showing permanent deformation by three-point bending test and correspond to specimen A in Fig.2.

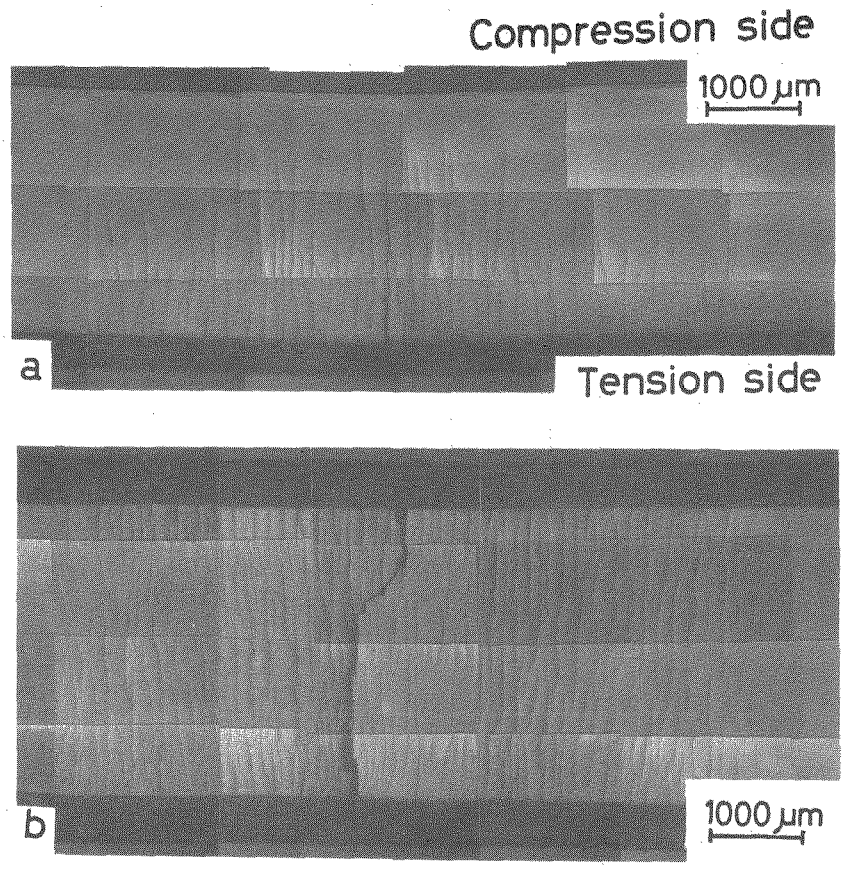

Fig.4 Potograph(a) and (b) show the crack configuration in a lateral surface and tension surface during three-point bending test, respectivery. These specimens correspond to A in Fig.2.

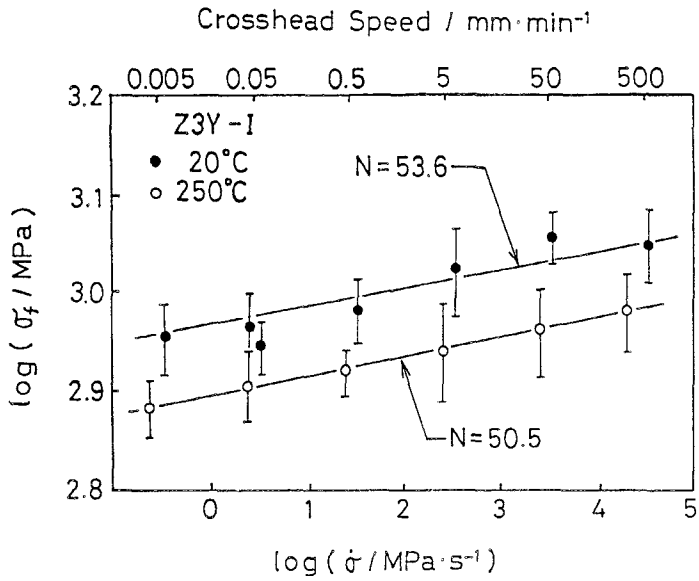

Fig.5. Relation between fracture stress (σ_f) and stressing rate ($\dot{\sigma}$) for 3 mol% Y_2O_3 containing tetragonal zirconia polycrystals (Z3Y-I).

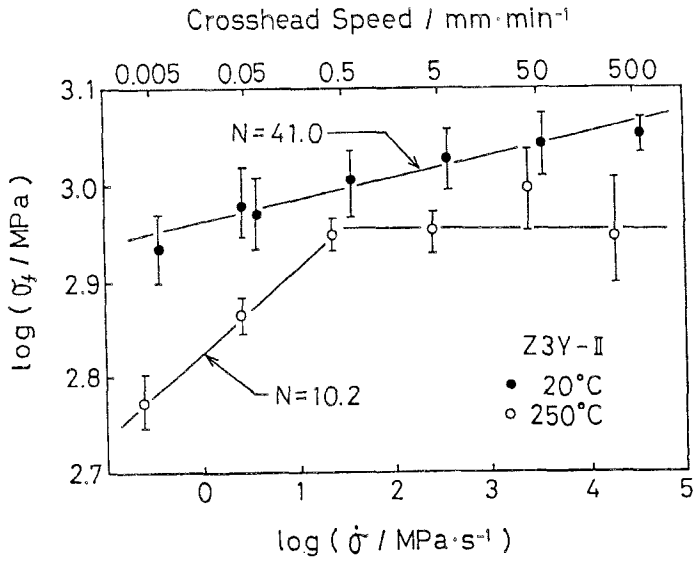

Fig.6. Relation between fracture stress (σ_f) and stressing rate ($\dot{\sigma}$) for 3 mol% Y_2O_3 containing tetragonal zirconia polycrystals (Z3Y-II).

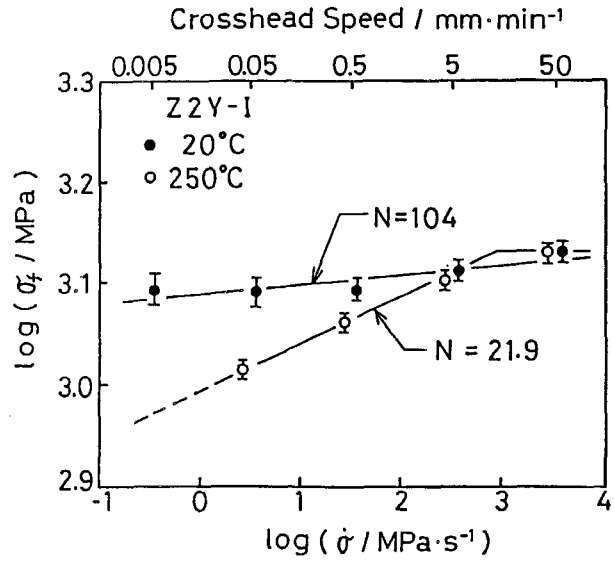

Fig.7. Relation between fracture stress (σ_f) and stressing rate ($\dot{\sigma}$) for 2 mol% Y_2O_3 containing tetragonal zirconia polycrystals (Z2Y-I).

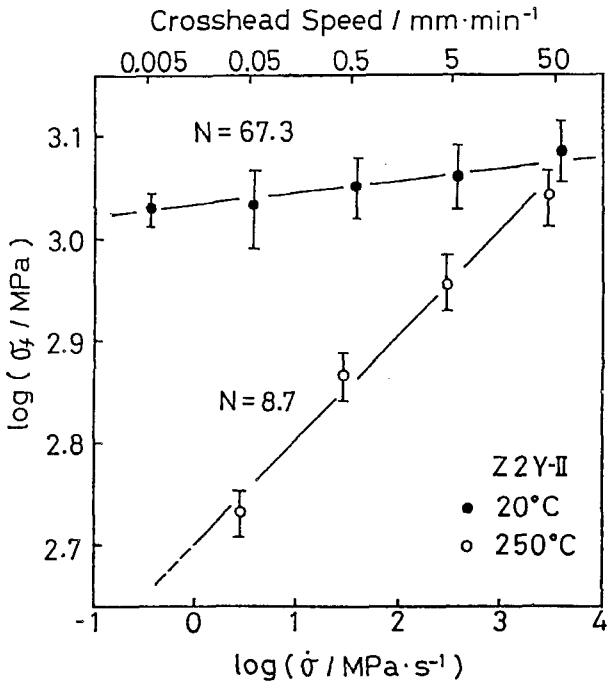

Fig.8. Relation between fracture stress (σ_f) and stressing rate ($\dot{\sigma}$) for 2 mol% Y_2O_3 containing tetragonal zirconia polycrystals (Z2Y-II).

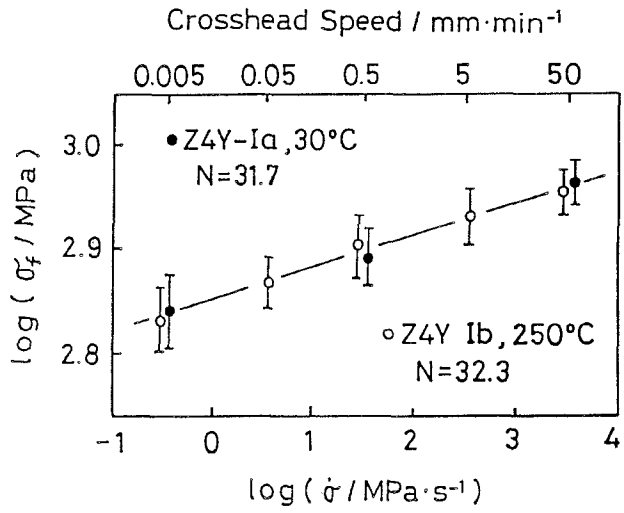

Fig.9. Relation between fracture stress (σ_f) and stressing rate ($\dot{\sigma}$) for 4 mol% Y_2O_3 containing tetragonal zirconia polycrystals (Z4Y-I a and I b).

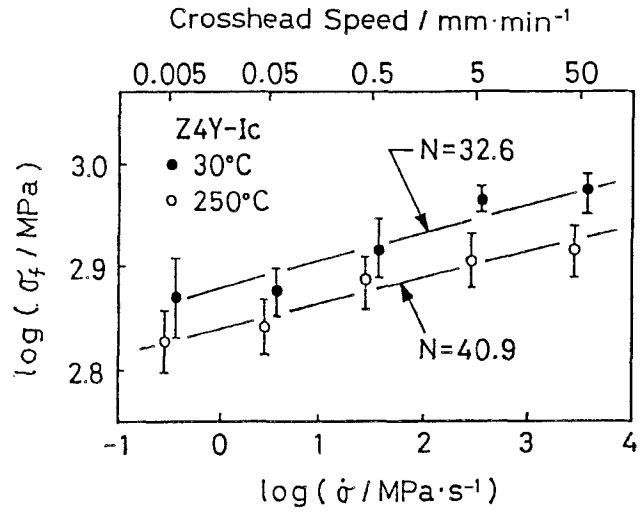

Fig.10. Relation between fracture stress (σ_f) and stressing rate ($\dot{\sigma}$) for 4 mol% Y_2O_3 containing tetragonal zirconia polycrystals (Z4Y-I c).

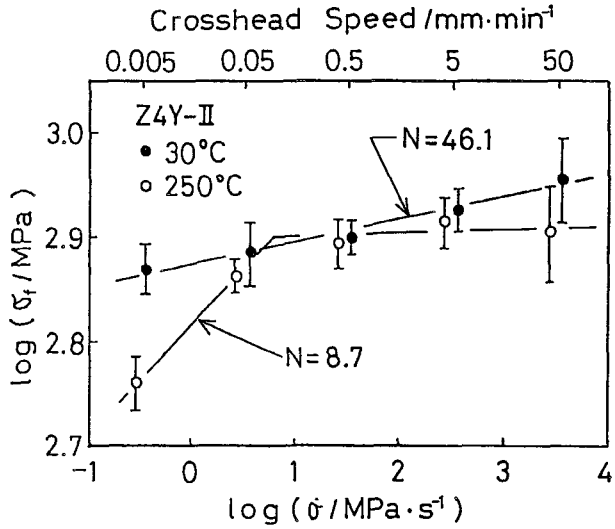

Fig.11. Relation between fracture stress (σ_f) and stressing rate ($\dot{\sigma}$) for 4 mol% Y_2O_3 containing tetragonal zirconia polycrystals (Z4Y-II).

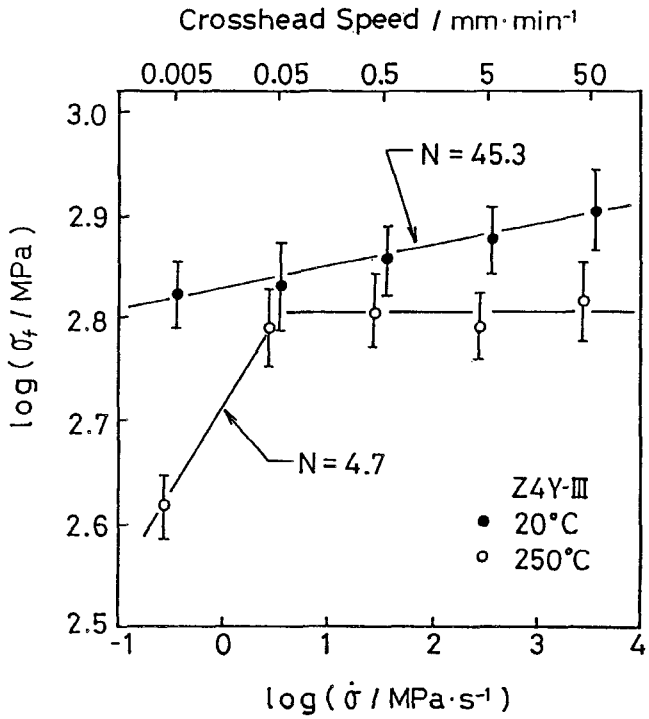

Fig.12. Relation between fracture stress (σ_f) and stressing rate ($\dot{\sigma}$) for 4 mol% Y_2O_3 containing tetragonal zirconia polycrystals (Z4Y-III).

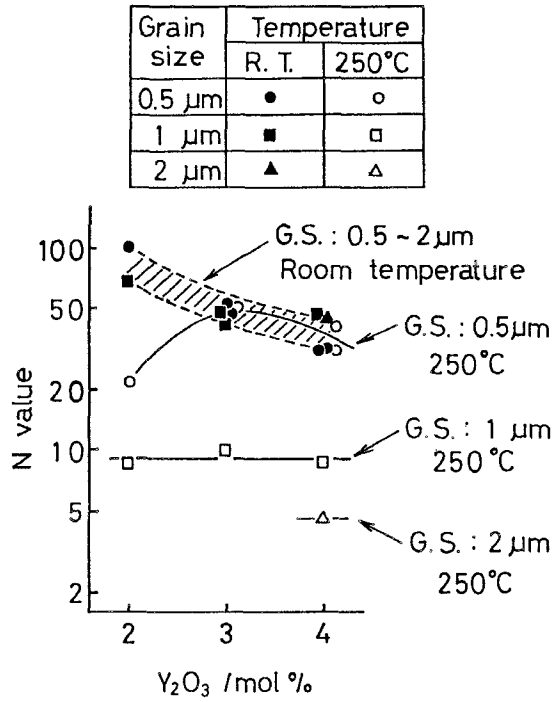

Fig.13. Relation between N values and Y_2O_3 contents for grain size groups (G.S.) of 0.5, 1.0 and 2.0μm.

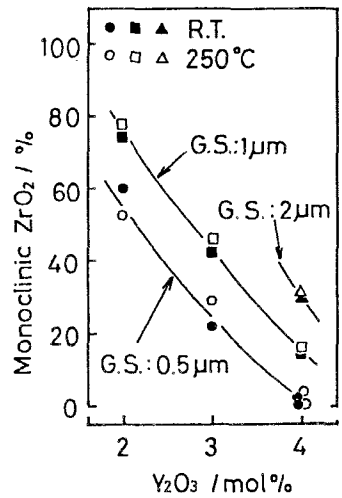

Fig.14. Relation between monoclinic zirconia contents on the fracture surface and Y_2O_3 contents for grain size groups (G.S.) of 0.5, 1.0 and 2.0μm. The symbols in this figure are the same as those in Fig.13

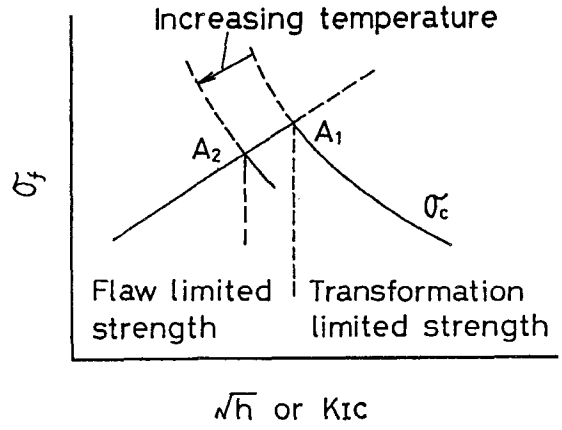

Fig.15. Schematic plots of fracture stress(σ_f) and critical transformation stress(σ_0) as a function of transformation zone size(h) or K_{IC}.

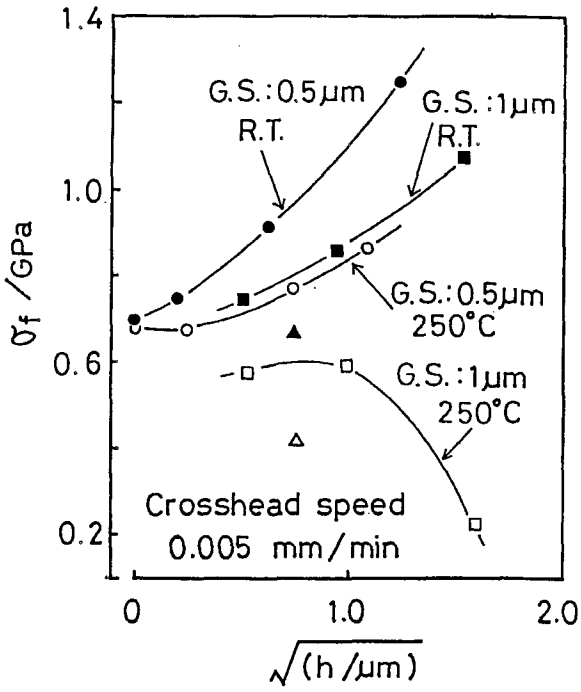

Fig.16. Plots of fracture stress(σ_f) of Y-TZP as a function of transformation zone size(h). G.S.: Grain size. The symbols in this figure are the same as those in Fig.13.

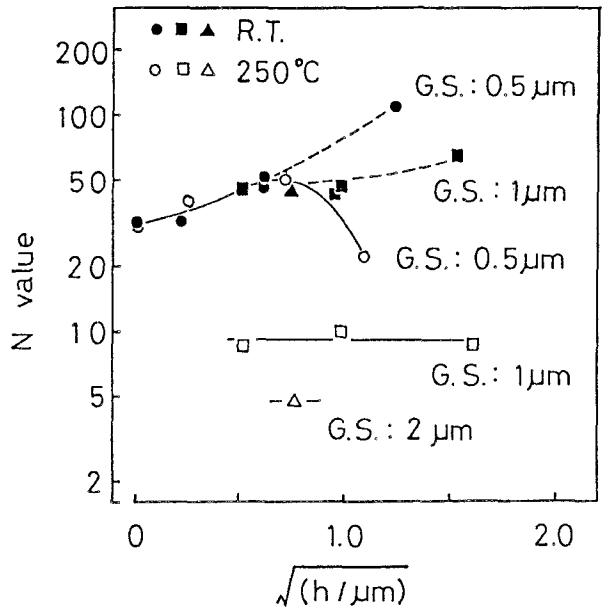

Fig.17 Relation between N values and transformation zone size(h) for grain size groups of 0.5, 1 and 2μm. R.T. : Room teperature. G.S. : Grain size. The symbols in this figure are the same as those in Fig.13.

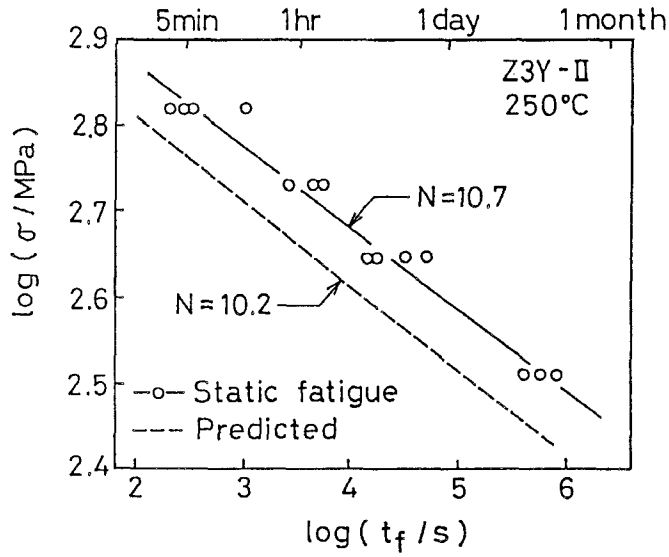

Fig.18 Relation between failure time(t_f) and applied stress(σ) for 3 mol%Y_2O_3 containing tetragonal zirconia polycrystals (Z3Y-II) at 250℃ (static fatigue). Broken lines represent the values estimated from dynamic fatigue data.

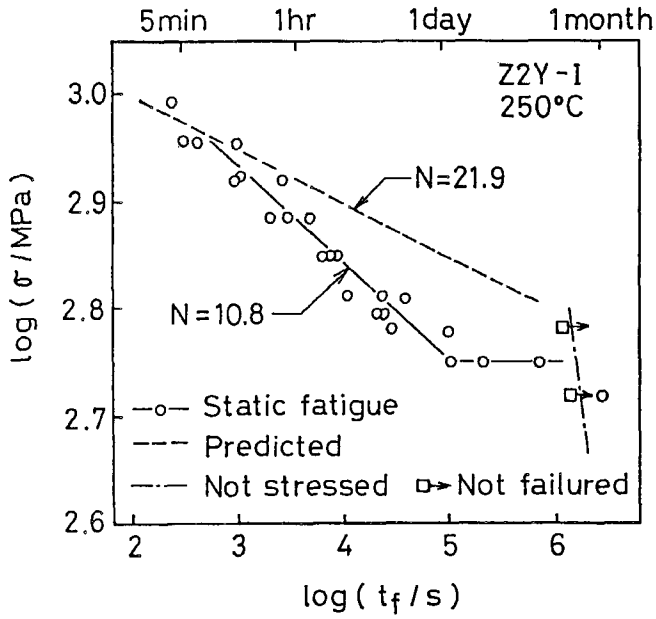

Fig.19 Relation between failure time(t_f) and applied stress(σ) for 2 mol% Y_2O_3 containing tetragonal zirconia polycrystals (Z2Y-I) at 250℃ (static fatigue). Broken lines represent the values estimated from dynamic fatigue data.

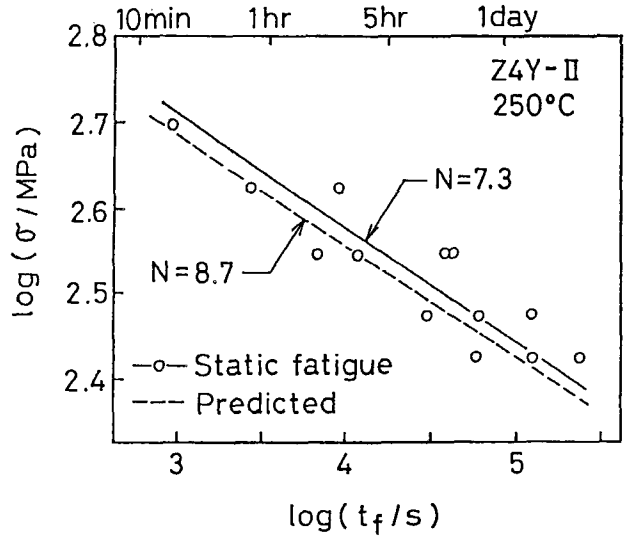

Fig.20 Relation between failure time(t_f) and applied stress(σ) for 4 mol%Y_2O_3 containing tetragonal zirconia polycrystals (Z4Y-II) at 250℃ (static fatigue). Broken lines represent the values estimated from dynamic fatigue data.

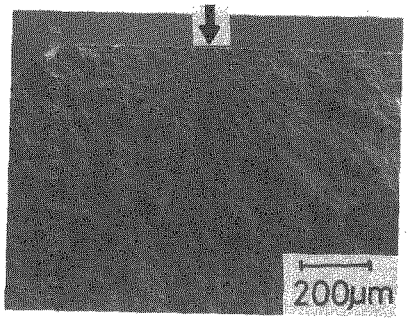

Fig.21 Fracture surface of 3 mol% Y_2O_3 containing tetragonal zirconia polycrystals(Z3Y-I) tested at stressing rate of 33.6 MPa/s (crosshead speed : 0.5mm/min.) at 20℃ (dynamic fatigue). Arrows show the fracture origin.

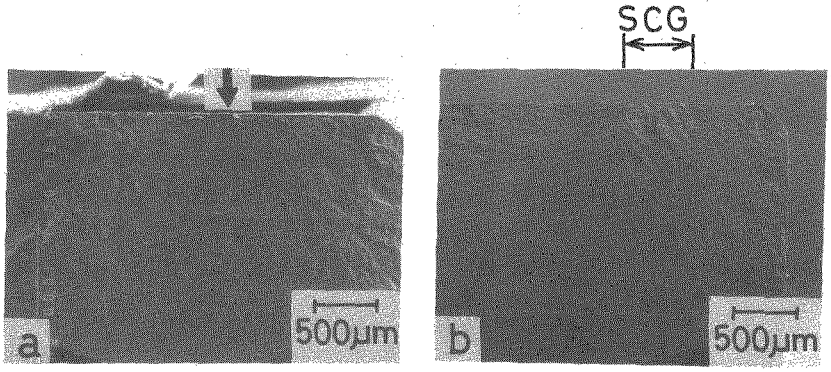

Fig.22 Fracture surface of 3 mol% Y_2O_3 containing tetragonal zirconia polycrystals tested at the lower stressing rate of 0.336 MPa/s(crosshead speed : 0.005mm/min.) at 250℃ (dynamic fatigue). A arrow shows the fracture origin. (a) : Z3Y-I , (b) : Z3Y-II

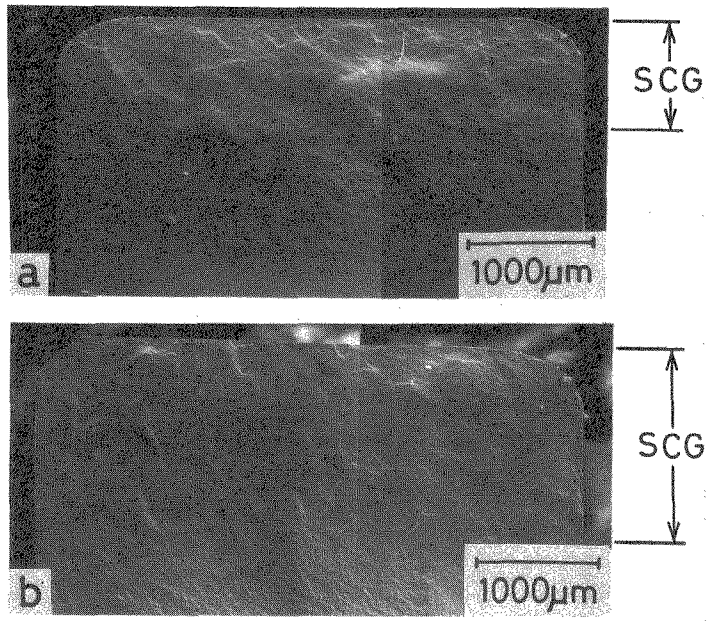

Fig.23 Fracture surface of 2 mol% Y_2O_3 containing tetragonal zirconia polycrystals(Z2Y-Ⅱ) at 250℃.
(a) Stressing rate : 3.02MPa/s
(crosshead speed 0.05mm/min).
(b) Stressing rate : 0.302MPa/s
(crosshead speed 0.005mm/min).

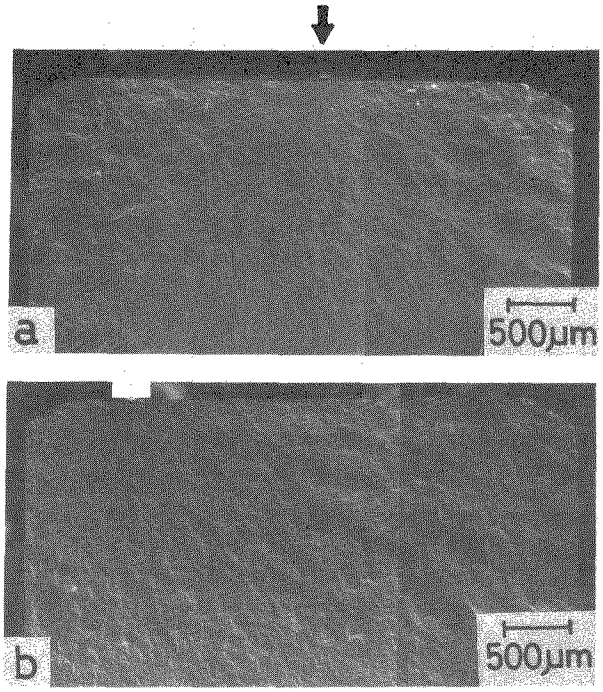

Fig.24 Fracture surface of 2 mol% Y_2O_3 containing tetragonal zirconia polycrystals(Z2Y-I) at 250℃.
(a) Stressing rate : 30.2MPa/s
(crosshead speed 0.5mm/min).
(b) Stressing rate : 0.302MPa/s
(crosshead speed 0.005mm/min).
Arrows show the fracture origin.

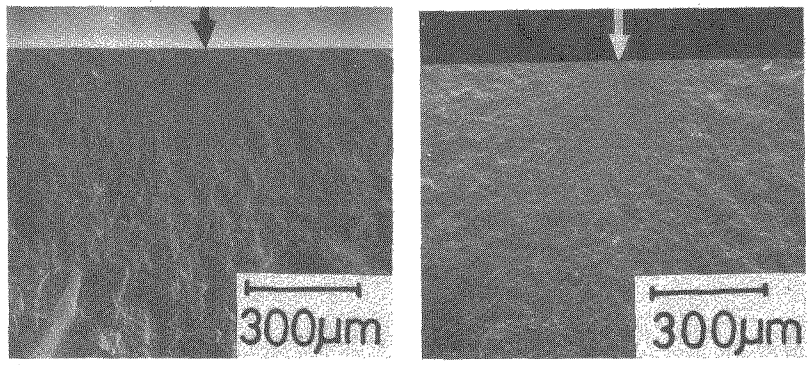

Fig.25 Fracture surface of 4 mol% Y_2O_3 containing tetragonal zirconia polycrystals after dynamic fatigue test at 250℃.
Stressing rate : 0.302MPa/s(crosshead speed : 0.005mm/min).
(a) : Z4Y-I c . (b) : Z4Y-II

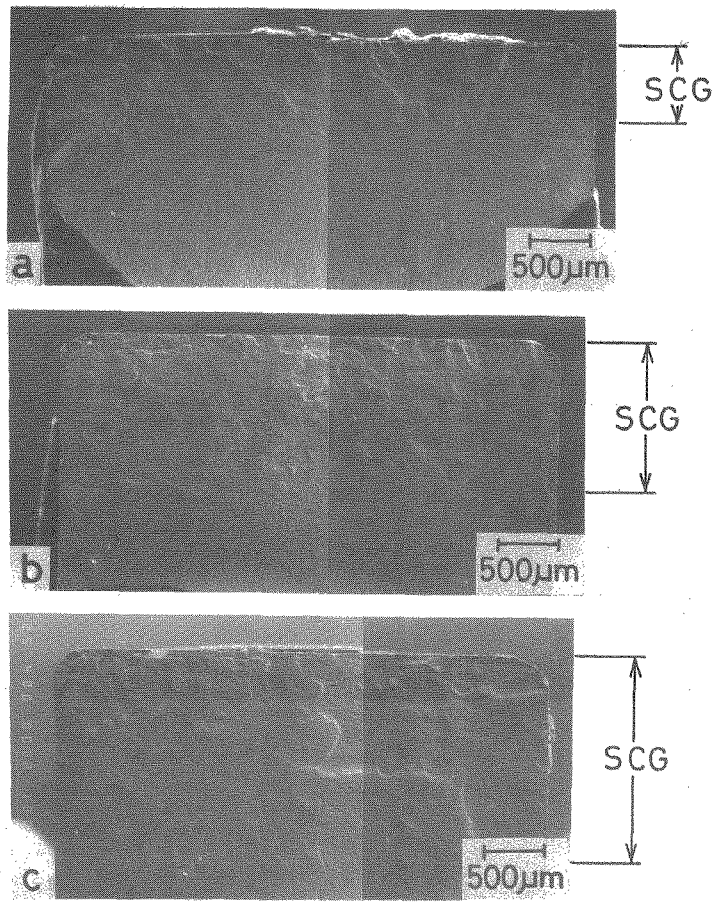

Fig.26 Fracture surface of 3 mol% Y_2O_3 containing tetragonal zirconia polycrystals(Z3Y-Ⅱ) after static fatigue test at 250℃.

(a) Applied stress : 541MPa, failure time : 1h 13min.

(b) Applied stress : 443Mpa, failure time : 9h 6min.

(c) Applied stress : 325MPa, failure time : 6day 8h 7min.

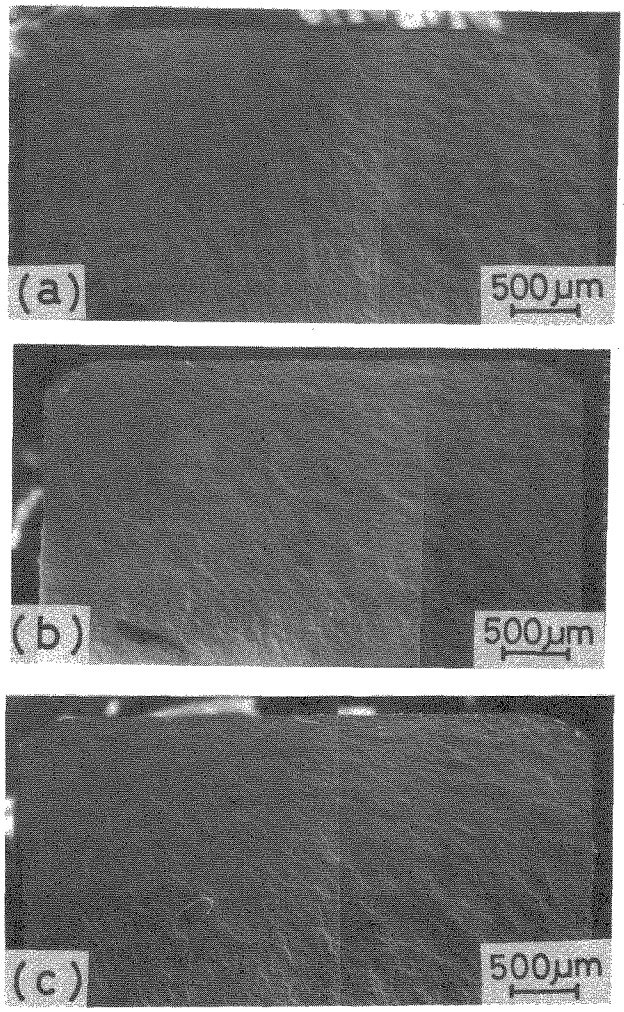

Fig.27 Fracture surface of 2 mol% Y_2O_3 containing tetragonal zirconia polycrystals(Z2Y-I) after static fatigue test at 250℃.

(a) Applied stress : 834MPa, failure time : 16min 13sec.

(b) Applied stress : 624Mpa, failure time : 6h 38min.

(c) Applied stress : 563MPa, failure time : 8day 2h 23min.

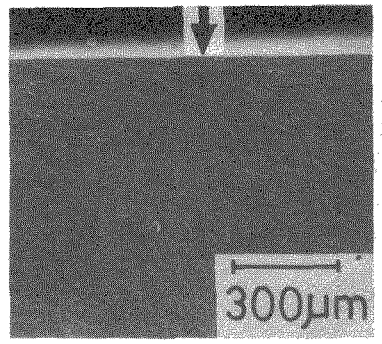

Fig.28 Fracture surface of 4 mol% Y_2O_3 containing tetragonal zirconia polycrystals(Z4Y-Ⅱ) after static fatigue test at 250℃.
Applied stress : 423MPa, failure time : 45min 51sec.

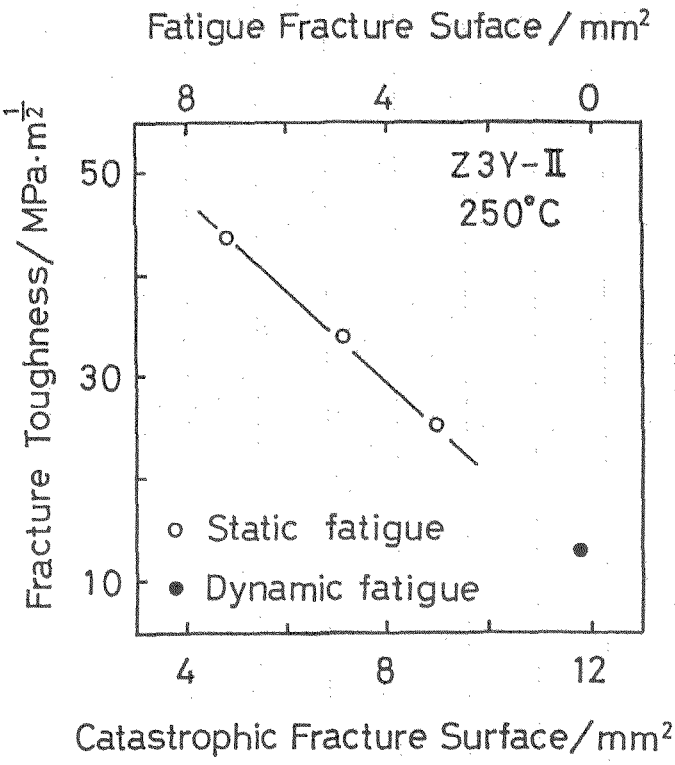

Fig.29 Fracture toughness estimated from static fatigue fracture surface(Fig.26 a, b and c) and dynamic fatigue fracture surface(Fig.22 b) at 250℃ (Z3Y-Ⅱ).

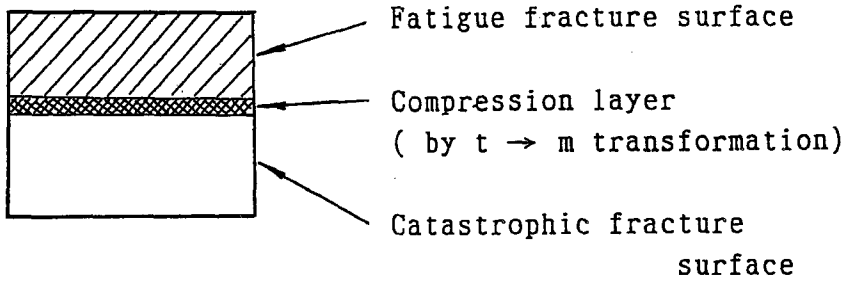

Fig.30 Compression layer at the tip of crack (schematic).

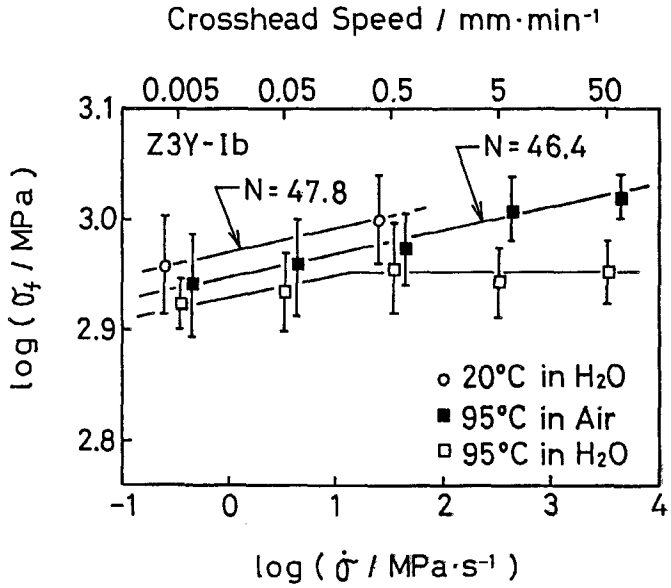

Fig.31 Relation between fracture stress (σ_f) and stressing rate ($\dot{\sigma}$) for 3 mol% Y_2O_3 containing tetragonal zirconia polycrystals (Z3Y-I b) in water.

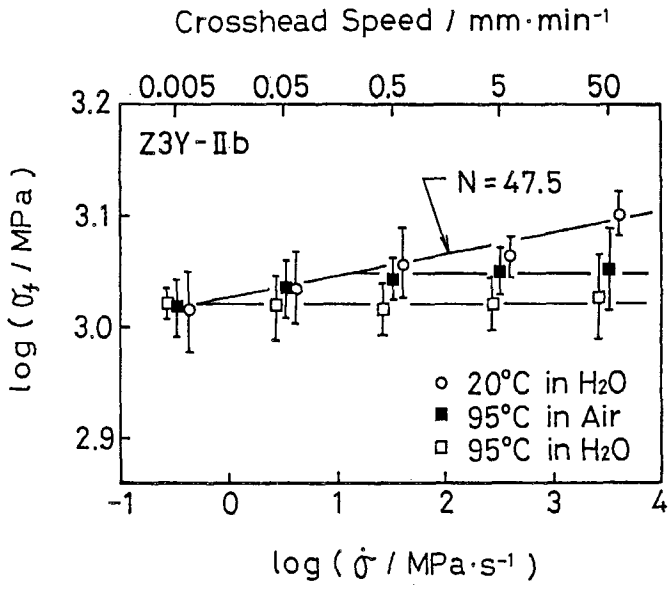

Fig.32 Relation between fracture stress (σ_f) and stressing rate ($\dot{\sigma}$) for 3 mol% Y_2O_3 containing tetragonal zirconia polycrystals (Z3Y-II b) in water.

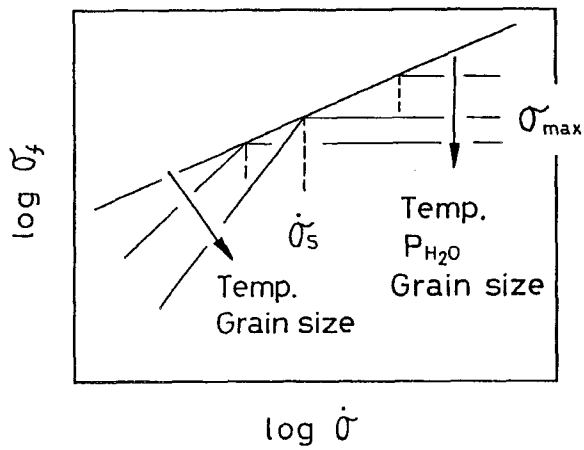

Fig.33 Schematic relationship between fracture stress (σ_f) and stressing rate ($\dot{\sigma}$) for Y-TZP.

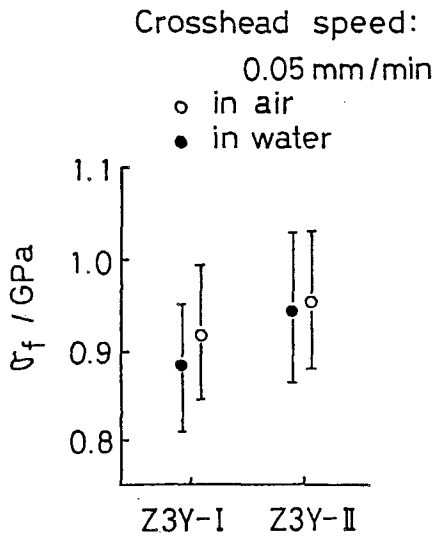

Fig.34 Comparison of strength in water with that in air at room temperature.